thickness) were prepared. These slices used for the RNA isolation without additional microdissection. Two to three slices were combined per each region, and total RNAs were prepared from this combined tissue sample using a Mini RNA isolation kit (Zymo Research, Orange, CA). The RNA solutions were treated with RNase-free DNase I (Ambion, Austin, TX) to digest contaminated DNA. After inactivation of DNase I, single-strand cDNA synthesis was performed using the Superscript II cDNA synthesis kit (Invitrogen, Gaithersburg, MD) with oligo(dT)$_{12-18}$ primers. This single-strand cDNA sample was used in quantitative PCR after digestion of RNA with RNase H. Quantitative PCR was performed with an Applied Biosystems (Foster City, CA) 7700 real-time PCR unit using the SYBR green premix and a primer set specific for each gene. β-actin sequence was used as an internal standard. The primer sets used to detect each gene are listed in supplemental Table 1 (available at www.jneurosci.org as supplemental material). The amplification efficiencies of GluR gene fragments by these eight primer sets were confirmed to be almost identical by checking the efficiency with a known concentration of template plasmid carrying each GluR gene fragment (including the amplification region). Also, the absence of any detectable cross-reactivity was confirmed by performing PCR, for example, using a flop-specific primer set and a plasmid carrying a fragment for a flip variant. The ΔCt value (Ct value of GluR-amplification minus the Ct value of β-actin amplification in the same sample) was calculated in each sample, and the relative expression of GluR to β-actin was expressed as a $2^{-\Delta Ct}$ value. The percentage of a flop variant was calculated, for example in the case of GluR1, by dividing the $2^{-\Delta Ct}$ value for GluR1-flop by the sum of those values for GluR1-flip and GluR1-flop.

Microinjection. Each male mouse (8–12 weeks old) was anesthetized with pentobarbital (50 mg/kg, i.p.) and affixed to the brain stereotaxic apparatus (Narishige Instruments, Tokyo, Japan). In the case of the mPFC injection, a single stainless-steel guide cannula (Eicom, Kyoto, Japan) was impaled into the brain so that its tip was positioned near the mPFC (anteroposterior, 2.10 mm from bregma; lateral, 0 mm; ventral, −1.71 mm). In the case of the amygdala injection, the guide cannulas were bilaterally impaled (anteroposterior, −1.22 mm from bregma; lateral ±2.83 mm; ventral, −4.00 mm). The cannulas were held in place with acrylic dental cement. A dummy cannula was inserted into the guide cannula to prevent clogging. Microinjection (0.2 μl per one individual) of PEPA (0.1 μg/μl) or vehicle (ACSF) was performed on day 2 or 3 after surgery. For microinjection, the dummy cannula was removed from the guide cannula, and a 28 gauge injection cannula, extending 0.5 mm from the tip of the guide cannula, was inserted under anesthesia with diethyl ether. The injection cannula was connected via Teflon tubing to a micro syringe (Hamilton Company, Reno, NV) driven by a micro infusion pump (WPI, Sarasota, FL). The injection rate was 0.05 μl/min. The injection cannula was left in position for an additional 2 min before withdrawal. Extinction training was performed 30 min after injection. After the behavioral test, mice were anesthetized with halothane and microinjected into the mPFC with 0.2 μl of bromophenol blue. The brain was isolated and sectioned (400 and 120 μm for the mPFC and amygdala, respectively) using a Vibratome 3000. Cannula location was assessed under a light microscope.

Statistical analysis. The statistical significance of differences among data groups was assessed using one-way measure ANOVA with Bonferroni/Dunn *post hoc* analysis or using the two-tailed Student's *t* test.

Results

PEPA injected before extinction training facilitates extinction learning for fear memory

First, we investigated the effects of PEPA on the extinction of fear memory. For this purpose, mice were trained to form contextual fear memory by loading electrical footshock in an operation box. At 24 h postconditioning, mice were re-exposed to the operation box for 360 s without footshock. In the present study, we called this first re-exposure "extinction training" (Fig. 1*A*). Mice were injected with PEPA (3, 10, and 30 mg/kg, i.p.) or vehicle 15 min before this extinction training (Fig. 1*A*). The vehicle-treated control mice displayed a severe freezing response during extinction training (Fig. 1*B*). Injection of PEPA reduced the duration of freezing in a dose-dependent manner (Fig. 1*B*), but statistical significance was obtained only in mice injected with 30 mg/kg PEPA [161.3 ± 16.8 s (n = 11), against the control value of 238.5 ± 15.8 s (n = 9); p = 0.002; Bonferroni/Dunn test]. After this extinction training, mice were returned to their home cage; at 72 h after the initial conditioning, they were again exposed to the operation box (without footshock). We called this second re-exposure the "extinction test" (Fig. 1*A*). The duration of the freezing response in this extinction test was significantly shorter in all four groups when compared with the respective values measured during extinction training (Fig. 1*C*) ($p < 0.001$ in the control and in mice injected with 3 or 30 mg/kg PEPA, and p = 0.007 in mice injected with 10 mg/kg PEPA; Bonferroni/Dunn test), suggesting that our experimental protocol could detect the extinction of fear memory. In mice injected with 30 mg/kg PEPA, the duration of the freezing response was 74.0 ± 6.8 s (n = 11), which differed significantly ($p < 0.001$, Bonferroni/Dunn test) from that measured for control mice (162.2 ± 13.0 s, n = 9) in the extinction test (Fig. 1*C*). Moreover, when compared with the control group, the reduction in the duration of the freezing response from extinction training to the extinction test did not change in mice injected with 3 or 10 mg/kg PEPA, but the reduction was highly significant in mice injected with 30 mg/kg PEPA (Fig. 1*D*) (n = 11; p = 0.005, Bonferroni/Dunn test). These results suggest that injection of 30 mg/kg PEPA 15 min before the extinction training facilitates the formation and subsequent development of extinction learning. This effect of PEPA depended on the extinction training because the effect of PEPA was not detected in the extinction test when the extinction training was omitted (Fig. 1*E*,*F*) [p = 0.969; vehicle (V) vs PEPA, n = 10]. This result suggests that PEPA during the extinction training is required for its action.

PEPA does not inhibit the initial retrieval of fear memory during extinction training

It has been reported that extinction learning is triggered by retrieval of fear memory (Ouyang and Thomas, 2005). Thus, we tested whether PEPA suppresses retrieval of fear memory. For this purpose, we analyzed the time course of freezing response when mice were exposed to the operation box during extinction training. PEPA was injected 15 min before extinction training, and the duration of freezing response was measured every 60 s during extinction training. The duration did not differ significantly for the initial two bins (p = 0.746 and 0.074 for bins 1 and 2, respectively) (Fig. 1*G*) between control and 30 mg/kg PEPA-injected mice. However, the duration was markedly shorter for PEPA-injected mice after the third bin (bins 3–5) (Fig. 1*G*), and the values for bins 3–5 were significantly smaller for the PEPA-injected mice (p = 0.002, 0.002, and 0.001, respectively, two-tailed Student's *t* test). In contrast, the pattern of the time course of freezing response was completely different in the case of the extinction test (Fig. 1*H*). The duration of freezing response for the PEPA-injected mice was significantly shorter at each time point compared with control mice ($p < 0.02$ for all points) (Fig. 1*H*). These results suggest that PEPA does not inhibit initial retrieval of fear memory.

The effect of PEPA on extinction learning is mediated by AMPA receptors

We tested whether the effect of PEPA on extinction learning is mediated by AMPA receptors. For this purpose, mice were injected with NBQX (1 mg/kg, s.c.), an antagonist of AMPA recep-

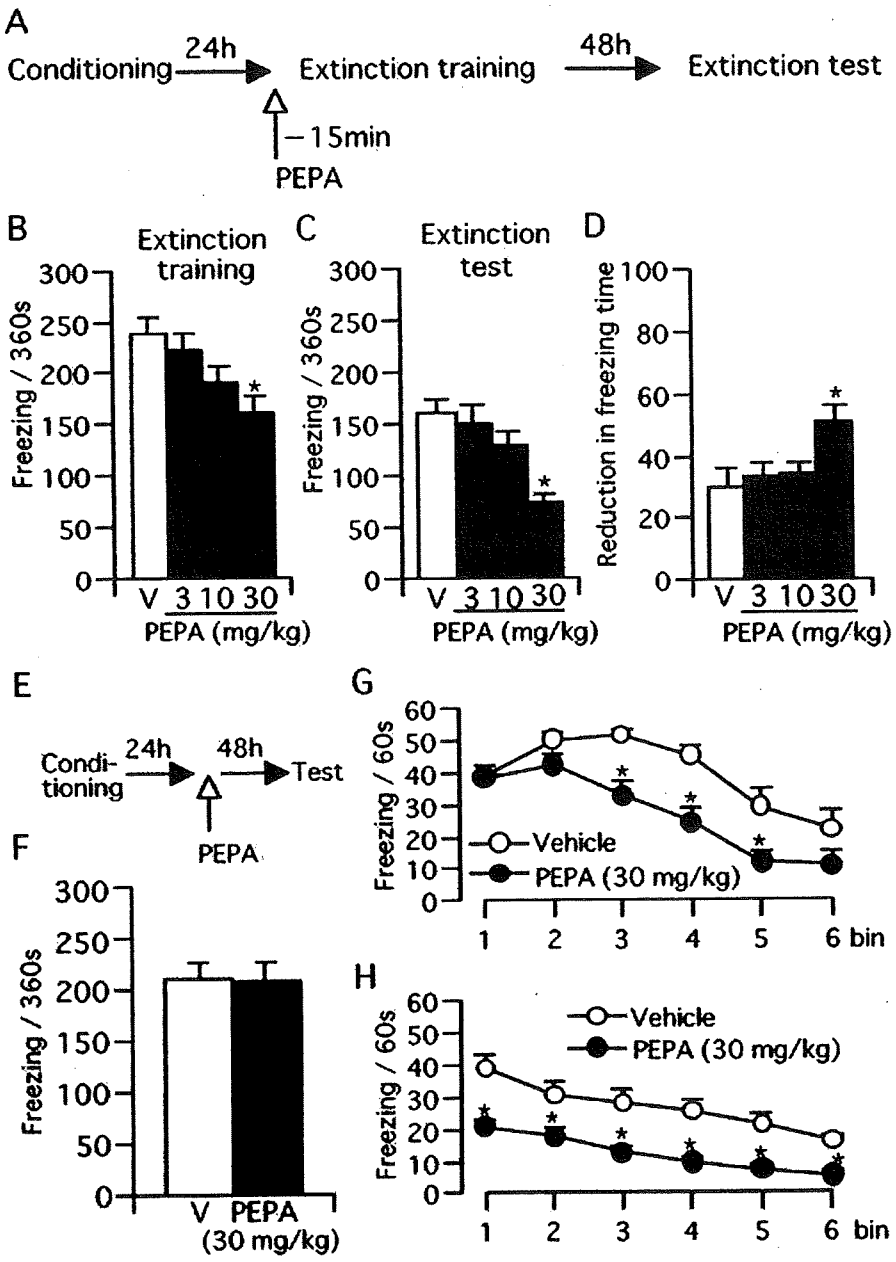

Figure 1. PEPA facilitates extinction learning. ***A***, Experimental design for ***B–D***. Mice were trained for the contextual fear conditioning and tested 24 h (extinction training) and 72 h (extinction test) later. PEPA or vehicle (V) was injected (i.p.) 15 min before extinction training. ***B***, ***C***, Dose-dependent reduction of freezing time during extinction training (***B***) and extinction test (***C***). Data represent mean + SEM (n = 9–11 for each group). ***D***, Reduction in freezing time between the extinction training and extinction test based on the data in ***B*** and ***C***. ***E***, Experimental design for ***F***. Mice were trained for the contextual fear conditioning and tested 72 h later (test) without extinction training. PEPA or vehicle were injected 24 h after conditioning. ***F***, PEPA did not reduce freezing time in the test when extinction training was skipped (n = 10 each). *Statistically significant (p = 0.002 vs V in ***B***; $p < 0.001$ vs V in ***C***, and p = 0.005 vs V in ***D***, Bonferroni/Dunn test). ***G***, ***H***, Changes in freezing time during the 360 s extinction training (***G***) and test (***H***) in groups injected with PEPA (30 mg/kg, n = 11) or vehicle (n = 9). Data used in ***B*** and ***C*** were reanalyzed for the time course of changes in freezing time (bin = 60 s). *Statistically significant (p = 0.002, 0.002, and 0.001 for bins 3–5, respectively, vs V in ***G***, and $p < 0.02$ for all vs V in ***H***, two-tailed Student's t test).

tors, 60 min before PEPA injection, and the extinction training and test were performed (Fig. 2*A*). We similarly injected saline (subcutaneously) as the control for NBQX treatment. The timing of injection and concentration of NBQX were determined by referring to a previous report (Lu and Wehner, 1997). The saline/PEPA-injected mice displayed a significantly shorter freezing time than saline/vehicle-injected mice in both the extinction training and test ($p < 0.001$ and p = 0.002 for training and test, respectively, Bonferroni/Dunn test) (Fig. 2*B*). These results were similar to those in Figure 1. The NBQX/PEPA-injected mice, however, displayed a significantly longer freezing response than saline/PEPA-injected mice (p = 0.004 and 0.001 for training and test, respectively, Bonferroni/Dunn test), and the values were comparable with those of control mice. The freezing response of NBQX/vehicle-injected mice did not differ significantly from saline/vehicle-injected mice (p = 0.614 and 0.784 for training and test, respectively, Bonferroni/Dunn test). These results suggest that pretreatment with NBQX antagonizes the action of PEPA on extinction learning.

PEPA does not influence locomotion and anxiolytic drug-sensitive behavior

Because augmented locomotion may be one of the indirect factors that attenuate freezing behavior, we examined whether PEPA stimulates locomotion. Mouse locomotion was measured in an open-field arena for 5 min, and 30 mg/kg PEPA was injected 15 min before the test. The locomotion, as assessed by the total distance the mouse traveled for 5 min, did not differ between control and PEPA-injected groups (Fig. 3*A*). In addition, because any compound that changes the anxiety state of mice may be difficult to assess with respect to its true effect on the inhibitory learning process (Bouton et al., 1990) (but see Castellano and McGaugh 1990), we tested the effect of PEPA on mouse behaviors, namely thigmotaxis and head dipping, that are sensitive to anxiolytic drugs such as benzodiazepines (Takeda et al., 1998; Kong et al., 2006). Thigmotaxis is a characteristic of walking close to the walls when a mouse is placed in an open-field arena (for review, see Prut and Belzung, 2003). Head-dipping is an exploratory behavior in which a mouse inserts its head into a hole prepared in an open-filed arena (Takeda et al., 1998). We compared these behaviors between mice injected with PEPA (30 mg/kg) or vehicle and found that the percentage of the time that mice spent at the perimeter in an open-field test (Fig. 3*B*) and the number of head-dipping behaviors in a hole-board test (Fig. 3*C*) were almost identical between PEPA- and vehicle-injected mice. These results suggest that PEPA does not induce detectable changes in locomotion or in the anxiety state of mice.

Neural circuit activation by PEPA is more potent in the mPFC than in the BLA and hippocampal CA1 field

We attempted to specify the brain region that is important for the effect of PEPA on extinction learning. As mentioned earlier, the

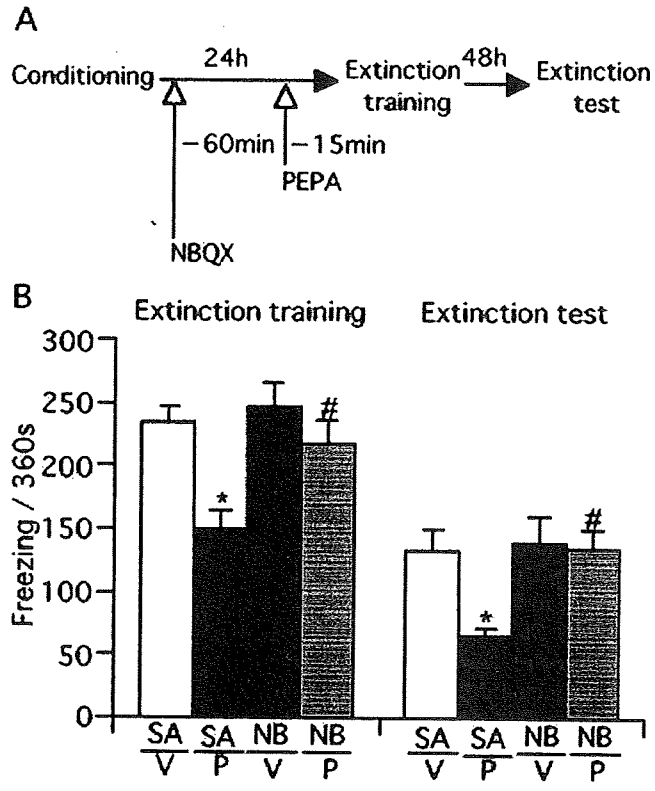

Figure 2. The effect of PEPA on extinction learning is mediated by AMPA receptors. ***A***, Experimental design. Mice were injected with saline (SA) or NBQX (NB, 1 mg/kg, s.c.) 60 min before vehicle (V) or PEPA (P; 30 mg/kg) injection (i.p.) and extinction training and testing were performed. ***B***, NBQX antagonizes the effect of PEPA on extinction learning. *Statistically significant ($p < 0.001$ and $p = 0.002$ vs SA/V in extinction training and test, respectively, Bonferroni/Dunn test; #$p = 0.004$ and 0.001 vs SA/P in extinction training and test, respectively, Bonferroni/Dunn test). Error bars indicate + SEM.

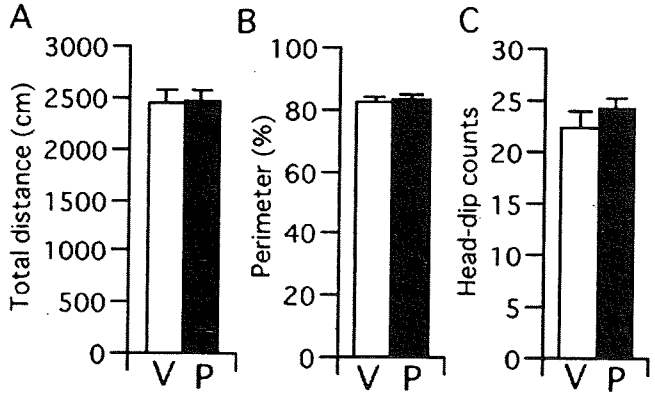

Figure 3. PEPA does not influence locomotion and anxiolytic drug-sensitive behavior. Mice were injected (i.p.) with vehicle (V) or PEPA (P; 30 mg/kg) 15 min before the open-field test and hole-board test. ***A***, ***B***, ***C***, Locomotion assessed by total distance that mice traveled for 5 min (***A***), the percentage of time that the mice spent in the perimeter of the open-field (***B***), and the number of head-dipping behaviors in the hole-board test (***C***). None of the values differed significantly between the groups injected with vehicle ($n = 6$ for all tests) or PEPA ($n = 7$ for all tests). Error bars indicate + SEM.

neural circuit consisting of the BLA, the hippocampus CA1/subiculum, and the mPFC is thought to be the main structure important for extinction learning of contextual fear memory. Thus, we tested the effect of PEPA on the synaptic response recorded from neurons in brain slices prepared from mouse mPFC, BLA, and hippocampal CA1 field.

Figure 4*A* shows synaptic currents recorded from layer V pyramidal cells in response to electrical stimulation of the mPFC layer II in mouse brain slices. Two types of synaptic current modulation were recorded when PEPA (50 μM) was applied to the slices. One was a simple augmentation of the synaptic currents, which we called type I modulation (Fig. 4*A*, mPFC type I). The AUB ratio of this type of modulation by PEPA was 1.25–2.26, and this type of modulation was observed in 11 of 17 cells recorded (65%). The other type involved potent epileptiform activity with long latency, which we called type II modulation (Fig. 4*A*, mPFC type II). Type II modulation was observed in 5 of 17 cells tested (29%). The epileptiform activity was not generated by the perfusion of PEPA alone without electrical stimulation of layer II, suggesting that this activity is elicited by synaptic activation. Application of AMPA receptor antagonist, CNQX (20 μM), completely abolished the epileptiform activity, as well as the initial small synaptic response, in cells showing type II modulation (Fig. 4*A*, mPFC type II), suggesting that AMPA receptors participated in the generation of the epileptiform activity. We defined the cases in which the AUB ratio was <1.1 as "no modulation" (NM), in which no obvious change in the current responses was evident. In the mPFC, 1 of 17 cells recorded was found to have NM. Augmentation of the synaptic currents by PEPA was dose dependent (Fig. 4*B*) in cells showing type I modulation, and 50 μM PEPA yielded a mean AUB ratio of 1.56 ± 0.11 ($n = 11$).

Figure 4*C* shows synaptic currents recorded from BLA pyramidal cells in response to electrical stimulation of the external capsule in mouse brain slices. When PEPA (50 μM) was applied to the slices, 11 of the 13 cases tested (85%) were found to have NM (AUB ratio, 0.91–1.09) (Fig. 4*C*, BLA NM). The remaining two cells (15%) exhibited the simple augmentation of the synaptic response (AUB ratio, 1.58 and 1.81), which is similar to type I modulation in the mPFC (Fig. 4*C*, BLA type I). In no case did PEPA cause the epileptiform activity.

Figure 4*D* shows synaptic currents recorded from neurons in the CA1 pyramidal layer in response to electrical stimulation of the stratum radiatum in mouse hippocampal slices. When PEPA (50 μM) was applied to the slices, 9 of the 12 cases tested (75%) were found to have NM (AUB ratio, 0.88–1.09) (Fig. 4*D*, CA1 NM). The remaining three cells (25%) exhibited the simple augmentation of the synaptic response (AUB ratio, 1.44, 2.11, and 2.92), which is similar to type I modulation in the mPFC (Fig. 4*D*, CA1-type I). In no case did PEPA cause the epileptiform activity. We applied cyclothiazide (CYZ), a flip splice variant-preferring potentiator of AMPA receptors (Partin et al., 1994), to the three cells that were found to have NM. Typical results are illustrated in Figure 4*D* (NM-CYZ); the application of CYZ very potently enhanced synaptic currents in these cells.

Figure 4*E* summarizes the effect of PEPA on synaptic currents in the three brain regions. PEPA showed much higher potency on synaptic currents in the mPFC than in the BLA and CA1. In particular, PEPA characteristically elicited epileptiform activity only in the mPFC. These electrophysiological data suggest that neural circuit activation by PEPA is more potent in the mPFC than in the BLA and hippocampal CA1 field.

Quantitative PCR analysis of AMPA receptor mRNA expression

As mentioned above, PEPA preferentially acts on flop variants and GluR3/4 subunits (Sekiguchi et al., 1997, 2002). In contrast, CYZ preferentially acts on flip variants (Partin et al., 1994). The potent augmentation by CYZ of synaptic currents that are insensitive to PEPA prompted us to hypothesize that AMPA receptors

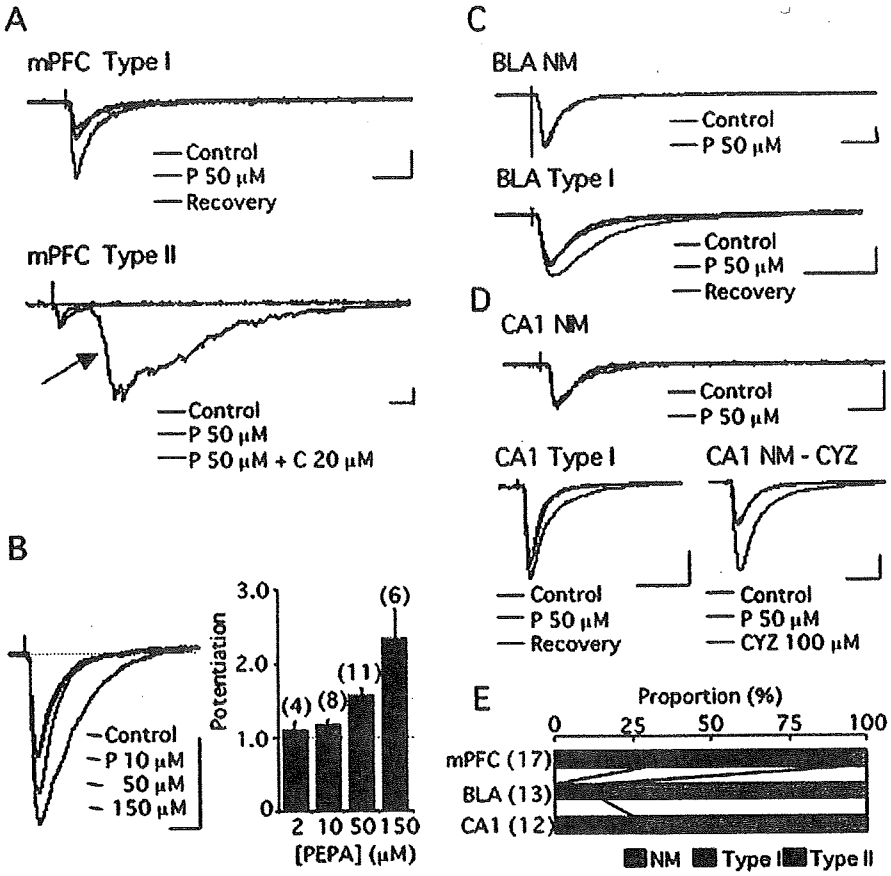

Figure 4. PEPA more potently activates the neural circuit in the mPFC than in the BLA or hippocampal CA1 field. *A*, mPFC-type I, An example of type I modulation by PEPA of synaptic currents recorded from layer V pyramidal cells in response to electrical stimulation of the mPFC layer II in mouse brain slices. *A*, mPFC-type II, An example of type II modulation by PEPA of similar synaptic currents. The arrow indicates epileptiform activity. C indicates CNQX. *B*, Dose-dependent augmentation of synaptic currents by PEPA in cells showing type I modulation. *C*, BLA-NM, An example of synaptic currents that were not affected by PEPA. NM, no modulation. The synaptic currents were recorded from a BLA pyramidal cell in response to electrical stimulation of the external capsule in mouse brain slices. BLA-type I, An example of type I modulation by PEPA of similar synaptic currents. *D*, CA1-NM, An example of synaptic currents that were not affected by PEPA. The synaptic currents were recorded from a neuron in the CA1 pyramidal layer in response to electrical stimulation of stratum radiatum in mouse hippocampal slices. CA1-type I, An example of type I modulation by PEPA of similar synaptic currents. NM-CYZ, An example of similar synaptic currents that were not affected by PEPA but potently enhanced by CYZ. Calibrations: 20 ms, 100 pA. *E*, Summary of the action of PEPA (50 μM) in the mPFC, BLA, and CA1-field (the total number of cells tested is shown in parentheses). The proportion of the cells exhibiting NM, type I, and type II modulations is indicated by color in each bar. Error bars indicate + SEM.

in the mPFC have subunit and splice variant compositions that are particularly sensitive to PEPA, which would explain why PEPA preferentially activates neural circuits in the mPFC. Indeed, it is reported that GluR3-flop, one of PEPA-preferring subunits, is relatively abundantly expressed in the rat PFC when compared with GluR1-flip, GluR1-flop, and GluR3-flip (Stine et al., 2001). To test this idea, we performed quantitative PCR for RNA samples prepared from mouse mPFC, the amygdala (including the BLA), and the hippocampus.

Figure 5*A* shows normalized expression levels of each AMPA receptor subunit in the three brain regions tested. The expression level of GluR3 was significantly higher in the mPFC than in the amygdala and hippocampus ($p = 0.017$ vs the amygdala, and $p < 0.001$ vs the hippocampus, two-tailed Student's t test). The expression level of GluR4 was significantly higher in the mPFC than in the hippocampus ($p < 0.001$, two-tailed Student's t test). Because PEPA prefers GluR3/4, it is possible that the higher electrophysiological activity of PEPA in the mPFC compared with the hippocampus is attributable to the higher relative expression level of GluR3/4 in the mPFC. In the case of the amygdala, however, the expression level of GluR4 was not significantly different from the mPFC and the difference in the expression level of GluR3 was not so remarkable as the case of the hippocampus. Thus, we compared the relative expression of flop variants between the mPFC and amygdala. As Figure 5*B* shows, the percentage of the flop variant in all subunits was higher in the mPFC than in the amygdala ($p < 0.001$ for GluR1, $p = 0.006$ for GluR2, $p = 0.009$ for GluR3, and $p = 0.012$ for GluR4, two-tailed Student's t test; data for four mice). Because PEPA preferentially acts on flop variants compared with flip variants, it is possible that more abundant expression of flop variants in the mPFC than in the amygdala contributes to the higher activity of PEPA in the mPFC than the BLA.

Intra-mPFC injection of PEPA facilitates extinction learning

The electrophysiological results obtained above suggested the strong participation of the mPFC in facilitating the action of PEPA on extinction learning. To confirm this, we microinjected PEPA into the mPFC of fear-conditioned mice and performed extinction training and testing (Fig. 6*A*). For comparison, we also conducted bilateral microinjection of PEPA into the amygdala (Fig. 6*A*) using a similar number of mice and the same concentration of PEPA. We could not observe any abnormal behaviors such as seizures in either of the mice injected with PEPA into the mPFC or amygdala. The location of the tip of injection cannulas in the mPFC is indicated in Figure 6*B*, and *C* shows the duration of freezing response of mice microinjected with vehicle or PEPA (0.02 μg) into the mPFC. The PEPA-injected mice ($n = 5$) showed significantly shorter freezing time than the vehicle-injected mice ($n = 6$) both in the extinction training and test ($p = 0.004$ and 0.029, respectively, two-tailed Student's t test). In both the extinction training and test, the reduction of freezing time by PEPA was similar between intraperitoneal injection of 30 mg/kg PEPA (Fig. 1*B*,*C*) and intra-mPFC injection (32.4% for i.p. and 32.3% for intra-PFC in extinction training; 54.4% for i.p. and 60.7% for intra-mPFC in the extinction test). Figure 6, *D* and *E*, shows the time course of freezing response of mice received intra-mPFC injection in the extinction training and test, respectively. The patterns of the time course were almost similar to those obtained in intraperitoneal injection (Fig. 1*G*,*H*). In contrast, the intra-amygdala injection of PEPA (Fig. 6*F* for the cannula location) did not significantly change the freezing time in either extinction training or extinction test when compared with vehicle-injected mice (Fig. 6*G*) [$p = 0.120$ and 0.250, vehicle-injected group ($n = 5$) vs PEPA-injected group ($n = 6$) in extinction training and extinction test, respectively, two-tailed Student's t test]. However, although not significant, mice injected

with PEPA into the amygdala showed shorter freezing time in mean both in extinction training and the extinction test (Fig. 6G). Therefore, these results suggest that PEPA induces more potent facilitation of extinction with injection into the mPFC than injection into the amygdala.

Discussion

The main finding of our present study is that extinction learning for contextual fear memory is facilitated by PEPA, a potentiator of AMPA receptors (Fig. 1). This facilitation occurs through AMPA receptors (Fig. 2) without preventing initial fear memory retrieval (Fig. 1). PEPA does not affect locomotion or anxiolytic drug-sensitive behavior of mice (Fig. 3). We also found that PEPA somewhat selectively and potently activates circuit activity in the mPFC (Fig. 4), and that an intra-mPFC injection of PEPA facilitates extinction much more potently than an intra-amygdala injection (Fig. 6), suggesting that the mPFC is a major site in which PEPA acts to facilitate fear extinction.

The amygdala and hippocampus play a central role in forming contextual fear memory (for review, see LeDoux, 2000; Maren, 2001). The information flow from the hippocampus CA1 field or subiculum to the BLA followed by that from the BLA to central amygdala (CeA) is thought to be necessary for contextual fear memory formation (Maren and Fanselow, 1995; for review, see LeDoux, 2000; Maren, 2001). The projection from CeA to the periaqueductal gray matter (PAG) is critical for the freezing response (LeDoux et al., 1988). In contrast, the excitatory projections from the mPFC to the amygdala play a critical role in extinction learning (Morgan et al., 1993; Morgan and LeDoux, 1995; Garcia et al., 1999; Quirk et al., 2000, 2003; Rosenkranz and Grace, 2001). There are two models on the mechanism underlying extinction by the projection (for review, see Sotres-Bayon et al., 2004). One is a model that the excitatory projection elicits feedforward inhibition for BLA principal neurons via BLA inhibitory interneurons (Rosenkranz and Grace, 2001), and another is a model that the projection elicits feedforward inhibition for CeA projection neurons via inhibitory neurons in the intercalated cell masses (Quirk et al., 2003). These inhibitions attenuate activation of CeA projection neurons, which suppress the CeA-PAG pathways to decrease the freezing response (for review, see Sotres-Bayon et al., 2004). Our present finding that a drug that potently activates the neuronal circuits in the mPFC facilitates extinction learning is in agreement with this significant role of the mPFC in extinction learning. In particular, it is characteristic that PEPA selectively elicits epileptiform activity in the mPFC. The generation of this type of activity increases spike firings, and the robust increment in spike firings in the infralimbic region of the mPFC reportedly occurs in response to re-exposure of rats to the CS (Milad and Quirk, 2002). Therefore, it is possible that PEPA facilitates extinction learning by enhancing the generation of epileptiform activity in the mPFC. This speculation is favored by previous reports which suggest no effect of intra-amygdala infusion of AMPA receptor antagonists on extinction (Falls et al., 1992; Lin et al., 2003). Extinction learning is triggered by retrieval of fear memory in response to the context presentation (Ouyang and Thomas, 2005), and the hippocampus CA1 field may be critical for contextual fear memory retrieval (Hall et al., 2001). Our result that PEPA does not prevent initial fear memory retrieval (Fig. 1G) can be explained by the low abundance of PEPA-sensitive neurons in the CA1 pyramidal cell layer.

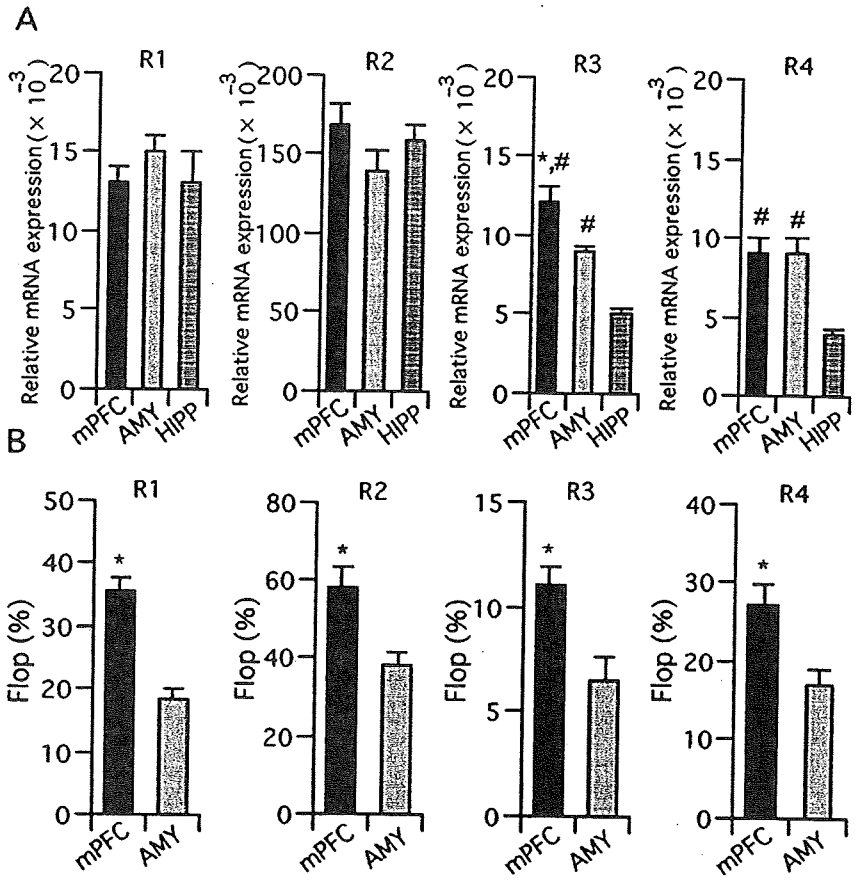

Figure 5. Quantitative PCR analysis of the expression of AMPA receptor mRNA. *A*, Expression levels of AMPA receptor subunit (GluR1–4) mRNAs in the mPFC, amygdala (AMY), and hippocampus (HIPP). The values were normalized to the value obtained for β-actin mRNA. $n = 4$ for mPFC and HIPP, and $= 3$ for AMY. *,#Statistically significant (*$p = 0.017$ vs AMY and #$p < 0.001$ vs HIPP in R3, #$p < 0.001$ vs HIPP in R4, two-tailed Student's *t* test). *B*, Percentage of flop variant mRNAs in GluR1–4 subunits in the mPFC and amygdala. $n = 8$ and 7 for mPFC and AMY, respectively. *Statistically significant ($p < 0.001$, $p = 0.006$, $p = 0.009$, and $p = 0.012$ vs AMY in R1, R2, R3, and R4, respectively). Error bars indicate + SEM.

Two factors can be pointed out for the relatively selective activation of the mPFC by PEPA. One is the relatively abundant expression of PEPA-preferring AMPA receptor subunits and splice variants in the mPFC, as shown by quantitative PCR (Fig. 5). The subunit and splice variant composition of AMPA receptors depends on the expression level of the subunits and variants in a cell. The expression of the GluR3/4 subunits, which are preferred by PEPA, is higher in the mPFC than in the hippocampus, and the expression of flop variants, which are preferred by PEPA, is higher in the mPFC than in the amygdala and, thus, it is reasonable to assume that PEPA-preferring AMPA receptors are much more abundant in the mPFC than in the CA1-field and amygdala. The potentiation of AMPA receptors by PEPA would be more pronounced under such conditions. Another factor underlying the relatively selective activation of the mPFC by PEPA is the specificity of neural circuits in the mPFC. It has been reported

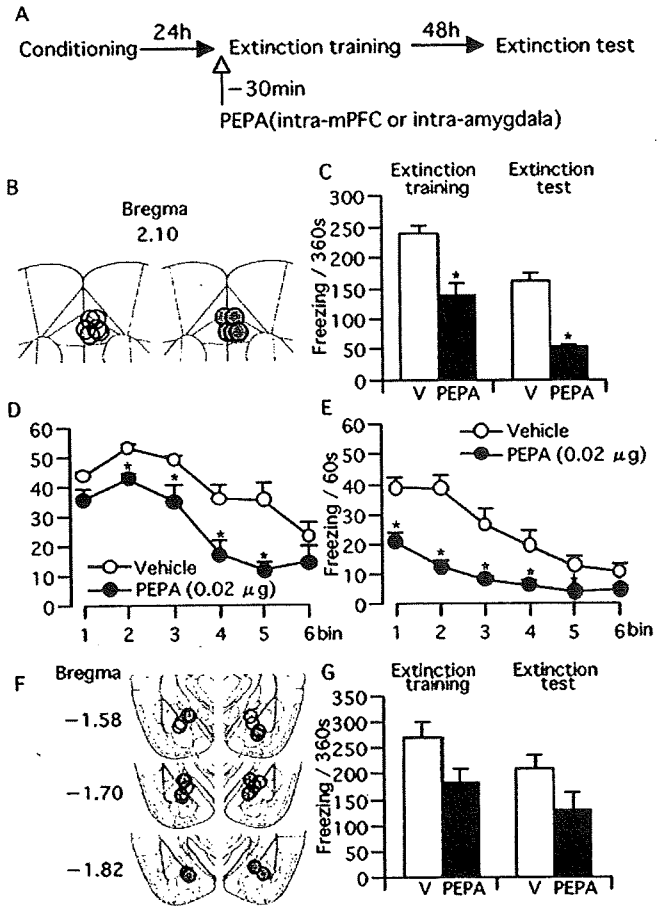

Figure 6. Intra-mPFC injection of PEPA (0.02 μg) 30 min before extinction training facilitates extinction learning. ***A***, Experimental design. Mice were trained for the contextual fear conditioning and tested 24 h (extinction training) and 72 h (extinction test) later. PEPA or vehicle (V) were microinjected into the mPFC or amygdala 30 min before extinction training. ***B***, Location of the injection cannulas within the mPFC. Open circles, Vehicle; shaded circles, PEPA. ***C***, Freezing time of mice microinjected with vehicle ($n = 6$) or PEPA ($n = 5$) into the mPFC in extinction training and test. *Statistically significant ($p = 0.004$ and 0.029 vs V in extinction training and test, respectively, two-tailed Student's *t* test). ***D***, ***E***, Changes in freezing time during the 360 s extinction training (***D***) and test (***E***) in groups injected with vehicle or PEPA. Data used in ***C*** were reanalyzed for the time course of changes in freezing time (bin = 60 s). *Statistically significant ($p = 0.004$, 0.017, 0.027, and 0.014 for bins 2–5, respectively, vs V in ***D***, and $p < 0.04$ for all vs V in ***H***, two-tailed Student's *t* test). ***F***, Location of the injection cannulas within the amygdala. Open circles, vehicle; shaded circles, PEPA. ***G***, Freezing time of mice microinjected with vehicle ($n = 6$) or PEPA ($n = 5$) into the amygdala in extinction training and test. The values in vehicle- and PEPA-injected groups are not significantly different in either extinction training or extinction test ($p = 0.120$ and 0.250 in extinction training and test, respectively, two-tailed Student's *t* test). Error bars indicate + SEM.

that layer V pyramidal neurons in the mPFC form a specific microcircuit (Wang et al., 2006). Specifically, 12% of the layer V pyramidal neurons form recurrent connections with other layer V pyramidal neurons, and 47% of the recurrent connections are reciprocal. In the hippocampus CA1 field, only 1% of the pyramidal cells form recurrent connections with each other (Deuchars and Thomson, 1996). The abundant recurrent connections among layer V pyramidal neurons can thus elicit population firings of connected pyramidal neurons in response to excitatory inputs. Under this condition, the PEPA-mediated enhancement of excitatory synaptic responses in layer V pyramidal neurons would increase the proportion of neurons that generate action potentials, which facilitates population firings through the activation of recurrent connections. The characteristic feature of PEPA action in the mPFC, namely the generation of epileptiform activity, can be explained by the presence of this amplification cascade based on the circuit characteristics of the mPFC.

In the present study, subcutaneous injection of NBQX alone did not affect extinction (Fig. 2). This, however, does not necessarily mean that intact (basic) activity of AMPA receptors in the mPFC is not important for extinction. The timing and dose of NBQX administration has not been examined in detail in the present study. Moreover, a higher dose of NBQX such as 30 mg/kg is reported to affect locomotion in rats (Danysz et al., 1994). Therefore, it seems that more detailed analysis including the intra-mPFC infusion of AMPA receptor antagonists is needed to establish the role of intact activity of AMPA receptors in extinction.

It has been reported that the function of the medial and orbital PFCs is attenuated during PTSD symptom provocation (Bremner, 1999) and that the function of the anterior cingulate cortex, a subregion of mPFC, in PTSD patients is reduced during extinction training for conditioned stimuli (Bremner et al., 2005). The reduction in the volume of the mPFC and attenuation in the reactivity of the mPFC in PTSD patients also has been reported (Shin et al., 2006). Given that the mPFC plays a crucial role in extinction learning, as mentioned above, a compound such as PEPA that facilitates extinction learning through the activation of the mPFC constitutes a potential drug candidate for CBT for complex anxiety disorders such as PTSD. To date, D-cycloserine (an NMDA receptor agonist/potentiator) (Walker et al., 2002), yohimbine (an α2-adrenoceptor antagonist) (Cain et al., 2006), AM404 (an inhibitor of endogenous cannabinoid breakdown and reuptake) (Chhatwal et al., 2005), and sulpiride (a D2 dopamine receptor antagonist) (Ponnusamy et al., 2005) have been reported to facilitate extinction learning for fear memory. These drugs are thought to facilitate the inhibitory association between the US and CS within the amygdala, but there is no drug that is specified to act on the mPFC. In fact, intra-amygdala injection of D-cycloserine is sufficient to facilitate extinction learning. Therefore, our results, especially those obtained from the intra-mPFC and intra-amygdala microinjections of PEPA, suggest the first example of a compound that facilitates extinction learning by mainly acting on the mPFC. Thus, PEPA (or its derivatives or similar compounds) may provide the basis for the discovery of new drugs that facilitate extinction learning and CBT for psychiatric disorders such as PTSD.

References

Amat J, Baratta MV, Paul E, Bland ST, Watkins LR, Maier SF (2005) Medial prefrontal cortex determines how stressor controllability affects behavior and dorsal raphe nucleus. Nat Neurosci 8:365–371.

Berman DE, Dudai Y (2001) Memory extinction, learning anew, and learning the new: dissociations in the molecular machinery of learning in cortex. Science 291:2417–2419.

Blanchard RJ, Blanchard DC (1972) Innate and conditioned reactions to threat in rats with amygdaloid lesions. J Comp Physiol Psychol 81:281–290.

Bouton ME (2002) Context, ambiguity, and unlearning: sources of relapse after behavioral extinction. Biol Psychiatry 52:976–986.

Bouton ME, Kenney FA, Rosengard C (1990) State-dependent fear extinction with two benzodiazepine tranquilizers Behav Neurosci 104:44–55.

Bouton ME, Rosengard C, Achenbach GG, Peck CA, Brooks DC (1993) Effects of contextual conditioning and unconditional stimulus presentation on performance in appetitive conditioning. Q J Exp Psychol B 46:63–95.

Bremner JD (1999) Alterations in brain structure and function associated with post-traumatic stress disorder. Semin Clin Neuropsychiatry 4:249–255.

Bremner JD, Vermetten E, Schmahl C, Vaccarino V, Vythilingam M, Afzal N, Grillon C, Charney DS (2005) Positron emission tomographic imaging of neural correlates of a fear acquisition and extinction paradigm in

women with childhood sexual-abuse-related post-traumatic stress disorder. Psychol Med 35:791–806.
Cain CK, Blouin AM, Barad M (2006) Adrenergic transmission facilitates extinction of conditional fear in mice. Learn Mem 11:179–187.
Castellano C, McGaugh JL (1990) Effects post-training bicuculline and muscimol on retention: lack of state dependency. Behav Neural Biol 54:156–164.
Chhatwal JP, Myers KM, Ressler KJ, Davis M (2005) Regulation of gephyrin and $GABA_A$ receptor binding within the amygdala after fear acquisition and extinction. J Neurosci 22:7892–7902.
Danysz W, Essmann U, Bresink I, Wilke R (1994) Glutamate antagonists have different effects on spontaneous locomotor activity in rats. Pharmacol Biochem Behav 48:111–118.
Davis M, Whalen PJ (2001) The amygdala: vigilance and emotion. Mol Psychiatry 6:13–34.
Davis M, Myers KM, Chhatwal J, Ressler KJ (2006) Pharmacological treatments that facilitate extinction of fear: relevance to psychotherapy. NeuroRx 3:82–96.
Deuchars J, Thomson AM (1996) CA1 pyramid-pyramid connections in rat hippocampus in vitro: dual intracellular recordings with biocytin filling. Neuroscience 74:1009–1018.
Falls WA, Miserendino MJ, Davis M (1992) Extinction of fear-potentiated startle: blockade by infusion of an NMDA antagonist into the amygdala. J Neurosci 3:854–863.
Fanselow MS (1998) Pavlovian conditioning, negative feedback, and blocking: mechanisms that regulate association formation. Neuron 20:625–627.
Garcia R, Vouimba RM, Baudry M, Thompson RF (1999) The amygdala modulates prefrontal cortex activity relative to conditioned fear. Nature 402:294–296.
Hall J, Thomas KL, Everitt BJ (2001) Cellular imaging of zif268 expression in the hippocampus and amygdala during contextual and cued fear memory retrieval: selective activation of hippocampal CA1 neurons during the recall of contextual memories. J Neurosci 21:2186–2193.
Hestrin S, Nicoll RA, Perkel DJ, Sah P (1990) Analysis of excitatory synaptic action in pyramidal cells using whole-cell recording from rat hippocampal slices. J Physiol (Lond) 422:203–225.
Kong WX, Chen SW, Li YL, Zhang YJ, Wang R, Min L, Mi X (2006) Effects of taurine on rat behaviors in three anxiety models. Pharmacol Biochem Behav 83:271–276.
LeDoux JE (2000) Emotion circuits in the brain. Annu Rev Neurosci 23:155–184.
LeDoux JE, Iwata J, Cicchetti P, Reis DJ (1988) Different projections of the central amygdaloid nucleus mediate autonomic and behavioral correlates of conditioned fear. J Neurosci 10:1062–1069.
Lin CH, Yeh SH, Lu HY, Gean PW (2003) The similarities and diversities of signal pathways leading to consolidation of conditioning and consolidation of extinction of fear memory. J Neurosci 23:8310–8317.
Lu Y, Wehner JM (1997) Enhancement of contextual fear-conditioning by putative (±)-α-3-hydroxy-5-methylisoxazole-4-propionic acid (AMPA) receptor modulators and *N*-methyl-D-aspartate (NMDA) receptor antagonists in DBA/2J mice. Brain Res 768:197–207.
Maren S (2001) Neurobiology of Pavlovian fear conditioning. Annu Rev Neurosci 24:897–931.
Maren S, Fanselow MS (1995) Synaptic plasticity in the basolateral amygdala induced by hippocampal formation stimulation *in vivo*. J Neurosci 15:7548–7564.
Maren S, Quirk GJ (2004) Neuronal signaling of fear memory. Nat Rev Neurosci 5:844–852.
Mayer ML, Westbrook GL, Guthrie PB (1984) Voltage-dependent block by Mg^{2+} of NMDA responses in spinal cord neurones. Nature 309:261–263.
Milad MR, Quirk GJ (2002) Neurons in medial prefrontal cortex signal memory for fear extinction. Nature 420:70–74.
Morgan MA, LeDoux JE (1995) Differential contribution of dorsal and ventral medial prefrontal cortex to the acquisition and extinction of conditioned fear in rats. Behav Neurosci 109:681–688.
Morgan MA, Romanski LM, LeDoux JE (1993) Extinction of emotional learning: contribution of medial prefrontal cortex. Neurosci Lett 163:109–113.
Myers KM, Davis M (2002) Behavioral and neural analysis of extinction. Neuron 36:567–584.
Nakagawa T, Iino M, Sekiguchi M, Wada K, Ozawa S (1999) Potentiating effects of 4-[2-(phenylsulfonylamino)ethylthio]-2,6-difluoro-phenoxyacetamide (PEPA) on excitatory synaptic transmission in dentate granule cells. Neurosci Res 35:217–223.
O'Neill MJ, Bleakman D, Zimmerman DM, Nisenbaum ES (2004) AMPA receptor potentiators for the treatment of CNS disorders. Curr Drug Targets CNS Neurol Disord 3:181–189.
Ouyang M, Thomas SA (2005) A requirement for memory retrieval during and after long-term extinction learning. Proc Natl Acad Sci USA 102:9347–9352.
Ozawa S, Iino M, Abe M (1991) Excitatory synapse in the rat hippocampus in tissue culture and effects of aniracetam. Neurosci Res 16:6634–6647.
Partin KM, Patneau DK, Mayer ML (1994) Cyclothiazide differentially modulates desensitization of AMPA receptor splice variants. Mol Pharmacol 46:129–138.
Paxinos G, Franklin KB (2001) The mouse brain in stereotaxic coordinate, Ed 2. San Diego: Academic.
Ponnusamy R, Nissim HA, Babara M (2005) Systemic blockade of D2-like dopamine receptors facilitates extinction of conditioned fear in mice. Learn Mem 12:399–406.
Prut L, Belzung C (2003) The open field as a paradigm to measure the effects of drugs on anxiety-like behaviors: a review. Eur J Pharmacol 463:3–33.
Quirk GJ, Russo GK, Barron JL, Lebron K (2000) The role of ventromedial prefrontal cortex in the recovery of extinguished fear. J Neurosci 20:6225–6231.
Quirk GJ, Likhtik E, Pelletier JG, Pare D (2003) Stimulation of medial prefrontal cortex decreases the responsiveness of central amygdala output neurons. J Neurosci 23:8800–8807.
Rosenkranz JA, Grace AA (2001) Dopamine attenuates prefrontal cortical suppression of sensory inputs to the basolateral amygdala of rats. J Neurosci 21:4090–4103.
Sekiguchi M, Fleck MW, Mayer ML, Takeo J, Chiba Y, Yamashita S, Wada K (1997) A novel allosteric potentiator of AMPA receptors: 4-2-(phenylsulfonyl-amino)ethylthio-2,6-difluorophenoxyacetamide. J Neurosci 15:5760–5771.
Sekiguchi M, Takeo J, Harada T, Morimoto T, Kudo Y, Yamashita S, Kohsaka S, Wada K (1998) Pharmacological detection of AMPA receptor heterogeneity by use of two allosteric potentiators in rat hippocampal cultures. Br J Pharmacol 123:1294–1303.
Sekiguchi M, Nishikawa K, Aoki S, Wada K (2002) A desensitization-selective potentiator of AMPA-type glutamate receptors. Br J Pharmacol 136:1033–1041.
Shin LM, Rauch SL, Pitman RK (2006) Amygdala, medial prefrontal cortex, and hippocampal function in PTSD. Ann NY Acad Sci 1071:67–79.
Sommer B, Keinanen K, Verdoorn TA, Wisden W, Burnashev N, Herb A, Kohler M, Takagi T, Sakmann B, Seeburg PH (1990) Flip and flop: a cell-specific functional switch in glutamate-operated channels of the CNS. Science 249:1580–1585.
Sotres-Bayon F, Bush DEA, LeDoux JE (2004) Emotional perseveration: an update on prefrontal-amygdala interactions in fear extinction. Learn Mem 11:525–535.
Stine CD, Lu W, Wolf ME (2001) Expression of AMPA receptor flip and flop mRNAs in the nucleus accumbens and prefrontal cortex after neonatal ventral hippocampal lesions. Neuropsychopharmacology 24:253–266.
Takamatsu I, Sekiguchi M, Wada K, Sato T, Ozaki M (2005) Propofol-mediated impairment of CA1 long-term potentiation in mouse hippocampal slices. Neurosci Lett 389:129–132.
Takeda H, Tsuji M, Matsumiya T (1998) Changes in head-dipping behavior in the hole-board test reflect the anxiogenic and/or anxyolytic state in mice. Eur J Pharmacol 350:21–29.
Takeda H, Tsuji M, Miyamoto J, Matsuya J, Iimori M, Matsumiya T (2003) Caffeic acid produces antidepressive- and/or anxiolytic-like effects through indirect modulation of the alpha 1A-adrenoceptor system in mice. NeuroReport 14:1067–1070.
Walker DL, Ressler KJ, Lu KT, Davis M (2002) Facilitation of conditioned fear extinction by systemic infusions of D-cycloserine as assessed with fear-potentiated startle in rats. J Neurosci 22:2343–2351.
Wang Y, Markram H, Goodman PH, Berger TK, Ma J, Goldman-Rakic PS (2006) Heterogeneity in the pyramidal network of the medial prefrontal cortex. Nat Neurosci 9:534–542.

Journal of Neurochemistry, 2007, **101**, 1145–1152 doi:10.1111/j.1471-4159.2006.04432.x

Melanocortin receptor 4 is induced in nerve-injured motor and sensory neurons of mouse

Katsuhisa Tanabe,*,† Kazushige Gamo,*,‡ Shunsuke Aoki,§ Keiji Wada§ and Hiroshi Kiyama*

**Department of Anatomy and Neurobiology, Graduate School of Medicine, Osaka City University, Osaka, Japan*
†Department of Orthopaedic surgery, Nishinomiya Municipal Central Hospital, Nishinomiya, Japan
‡Department of Orthopaedic surgery, Graduate School of Medicine, Osaka University, Suita, Japan
§Department of Degenerative Neurological Diseases, National Institute of Neuroscience, NCNP, Kodaira, Japan

Abstract

We previously identified melanocortin receptor 4 (MC4R) in a search for genes associated with hypoglossal nerve regeneration. As melanocortins promote nerve regeneration after axonal injury, we investigated whether MC4R functions as a key receptor for peripheral nerve regeneration. *In situ* hybridization revealed that MC4R mRNA is induced in mouse hypoglossal motor neurons after axonal injury, whereas mRNAs for MC1R, MC2R, MC3R, and MC5R are not expressed either before or after nerve injury. This result was confirmed by RT-PCR. The level of MC4R mRNA expression increased significantly from day 3 after axotomy, reached a peak on day 5, and decreased to the control level on day 14. Similar induction of MC4R was observed in axotomized mouse dorsal root ganglia (DRGs). MC4R mRNA expression was induced exclusively among the MCR family in the L4-6 DRG after sciatic nerve injury. We further examined whether alpha-melanocortin stimulating hormone (alpha-MSH) promotes neurite elongation via MC4R. In mouse DRG neuron culture, alpha-MSH significantly promoted neurite outgrowth at a concentration of 10^{-8} mol/L. This neurite-elongation effect was entirely inhibited by the addition of a selective MC4R blocker, JKC-363. Therefore, it is concluded that alpha-MSH could stimulate neurite elongation via MC4R in DRG neurons. The present results suggest that induction of MC4R is crucial for motor and sensory neurons to regenerate after axonal injury.

Keywords: alpha-melanocortin stimulating hormone, dorsal root ganglion, hypoglossal, peptide, regeneration.
J. Neurochem. (2007) **101**, 1145–1152.

Peripheral nerves can survive and regenerate after axonal injury. In order to elucidate the mechanism of nerve regeneration and to identify therapeutic strategies for nerve injury, systematic screening of the transcriptome and proteome is an effective strategy. We have previously performed screening assays such as differential display and expressed-sequence-tag analysis, using the cDNA library from nerve-injured motor nuclei, as well as proteomic analysis (Kiryu *et al.* 1995; Tanabe *et al.* 1998, 1999, 2000, 2003; Konishi *et al.* 2006). In those studies, we identified several molecules that are induced in response to peripheral nerve injury. By expressed-sequence-tag analysis, we identified an increase in the amount of melanocortin receptor 4(MC4R) mRNA in axotomized hypoglossal nuclei (Tanabe *et al.* 1999). Melanocortin receptors (MCRs) have five subtypes, MC1R–MC5R (Starowicz and Przewlocka 2003). Although MC2R is a specific receptor for adrenocorticotropic hormone (ACTH) in the adrenal cortex, MC1R, MC3R, MC4R, and MC5R are able to bind to all melanocortins [ACTH, alpha-melanocortin stimulating hormone (MSH), beta-MSH, and gamma-MSH]. Melanocortins are involved in multiple neural functions such as regulation of food intake, pain, stress, and body temperature. Among them, alpha-MSH has been reported to promote nerve regeneration in some studies. In neuronal cell culture, alpha-MSH stimulates the neurite outgrowth of Neuro 2A cells (a neuronal cell line), neonatal

Received September 11, 2006; revised manuscript received December 4, 2006; accepted December 27, 2006.

Address correspondence and reprint requests to Hiroshi Kiyama, Department of Anatomy and Neurobiology, Osaka City University Graduate School of Medicine, 1-4-3 Asahimachi, Abenoku, Osaka 545-8585, Japan. E-mail: kiyama@med.osaka-cu.ac.jp

Abbreviations used: ACTH, adrenocorticotropic hormone; DRG, dorsal root ganglion; MCR, melanocortin receptor; MSH, melanocortin stimulating hormone.

dorsal root ganglion (DRG) neurons, fetal spinal cord cells, and neonatal corticospinal neurons (Van der Neut *et al.* 1988; van der Neut *et al.* 1992; Peulve *et al.* 1994; Adan *et al.* 1996; Joosten *et al.* 1996). In Neuro 2A cells, the neurite outgrowth stimulating effect of alpha-MSH is inhibited by a MC4R antagonist, suggesting that MC4R mediates neurite elongation due to alpha-MSH (Adan *et al.* 1996). In animal studies, exogenous alpha-MSH rapidly increases the number of myelinating fibers and reduces the recovery period of sensory and motor function after sciatic nerve injury (Bijlsma *et al.* 1983; Verhaagen *et al.* 1986; Dekker 1988). By contrast, administration of an alpha-MSH antagonist decreases the amount of functional recovery in animals (Plantinga *et al.* 1995). In spinal cord injury, alpha-MSH enhances spinal neurite outgrowth and improves functional recovery (Lankhorst *et al.* 1999).

In order to identify changes in the levels of MCR mRNAs in neurons in response to axonal injury, we examined the mRNA expression profile of all five MCRs in axotomized motor neurons. In addition, the expression level of MCR mRNAs was also examined in mouse L4-6 DRGs after sciatic nerve injury. Finally, the role of MC4R in the axonal outgrowth of DRG neurons was studied using a selective MC4R blocker, JKC-363.

Materials and methods

Animal operations

Adult male 8-week-old C57/BL6 mice (Nihon SLC, Hamamatsu, Japan) were deeply anesthetized with pentobarbital (0.03–0.05 mg/g body weight) and the right hypoglossal nerve or the left sciatic nerve was cut. At time points ranging from 1 day to 8 weeks following nerve injury, mice were deeply anesthetized with diethyl ether and the brains or bilateral L4-6 DRGs were extracted and fresh frozen.

Reverse transcription-PCR analysis

cDNA was made from the extracted hypoglossal nuclei and L4-6 DRGs, and RT-PCR was performed using paired primers for MC1R (bp630–649 and bp1101–1121, X65635), MC2R (bp 135–155 and bp 584–604, D31592), MC3R (bp 125–145 and bp 543–563, X74983), MC4R (bp 24–43 and bp 551–570, U08354), and MC5R (bp 1792–1811 and bp 2255–2273, AF201662), as previously described (Kiryu-Seo *et al.* 2005).

In situ hybridization

In situ hybridization was performed on coronal brain sections as described previously (Tanabe *et al.* 1998, 1999). cDNA for all five MCRs was amplified from C57/BL6 mouse tissues by PCR. MC1R cDNA (bp 59–627, X65635), MC2R cDNA (bp 476–1006, D31952), MC3R cDNA (bp 290–934, X74983), MC4R cDNA (bp478–965, NM016977), and MC5R cDNA (bp 24–570, U08354) were subcloned into the pGEM-T Easy vector (Invitrogen, Carlsbad, CA, USA). *In vitro* transcription from linearized plasmids was performed using T7 and SP6 RNA polymerase (Promega, Madison, WI, USA) and [α-^{35}S]UTP (DuPont NEN, Wilmington, DE, USA) to prepare both antisense and sense riboprobes. After hybridization to tissue sections, mRNA localization was assessed by both film and emulsion autoradiography. The signal density in the X-ray film was quantified with Adobe Photoshop software (Adobe, San Jose, CA, USA).

DRG neuron culture

We collected DRGs from 8–10-weeks-old C67/BL6 mice. Neurons were dissociated and cultured on poly-L-lysine-laminin coated coverglass, as previously described (Bonilla *et al.* 2002). Alpha-MSH (Sigma, St Louis, MO, USA) and/or the selective MC4R antagonist JKC-363 (cyclic [Mpr11, D-Nal14, Cys18, Asp22-NH2]-beta-MSH 11–22) (Sigma) were added immediately after cell spreading. Cells were cultured for 20 h and fixed with 4% formaldehyde.

Immunohistochemistry and assessment of neurite length

Fixed DRG cultures were permeabilized in 0.2% triton-X and neurites were visualized using anti-beta-tublin III antibody (Promega) and Alexa-488 anti-mouse IgG secondary antibody (Molecular Probes, Eugene, OR, USA). Micrographs of immunostained cells were captured using an Olympus AX70 light microscope and a CCD camera (Olympus, Tokyo, Japan), and the length of the longest neurite on each DRG neuron was measured using NIH Image software (Scion Corporation, Frederick, MD, USA). The mean length of the longest neurite per neuron was evaluated. We repeated the DRG culture more than three times per experiment to confirm the results.

Results

MC4R mRNA expression is induced in the hypoglossal nucleus after axotomy

In our previous gene screening study, we identified MC4R as a candidate gene whose mRNA expression was up-regulated in axotomized hypoglossal nuclei (Tanabe *et al.* 1999). Using RT-PCR, we examined the mRNA levels for all five MCRs in axotomized and control hypoglossal nuclei (Fig. 1). Among MCR family members, only MC4R mRNA could be identified in normal hypoglossal nuclei using 25 PCR cycles; the level of MC4R mRNA was higher in axotomized hypoglossal nuclei. To identify the cell types expressing MC4R mRNA, we performed *in situ* hybridization. Brain sections were hybridized with cRNA probes against all five MCR mRNAs 5 days after nerve injury (Fig. 2). On film autoradiograms, a hybridization signal was observed only for MC4R mRNA, and other MCR mRNAs were not detected in either control or injured hypoglossal nuclei (Fig. 2a). Prominent MC4R mRNA expression was observed in the injured hypoglossal nucleus (Fig. 2a arrow), but only a faint hybridization signal was observed in the control hypoglossal nucleus. Signal for MC4R mRNA was also observed in the bilateral dorsal motor nuclei of vagus where the intact neurons existed. Emulsion autoradiography showed hybridization signal mainly over large cells, suggesting that MC4R

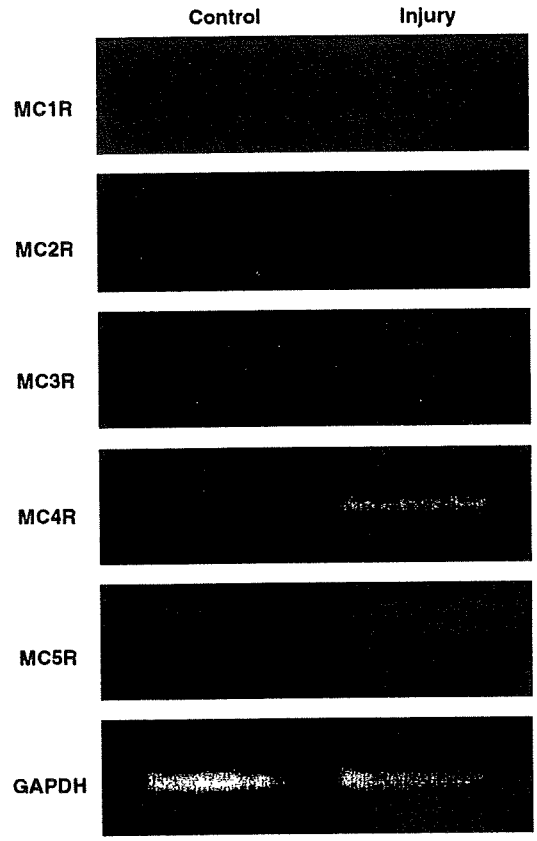

Fig. 1 RT-PCR study of the melanocortin receptor family in hypoglossal nuclei, 5 days after the right hypoglossal nerve injury. After 25 PCR cycles, expression of melanocortin receptor (MCR) MC4R mRNA was detected in the intact nucleus and increased in the nucleus on the injured side. However, mRNAs for the other MCRs were not seen in either nucleus. Expression of GAPDH was used as an internal control.

mRNA-positive cells were motor neurons rather than glial cells such as astrocytes and microglia (Fig. 2b).

Expression profile of MC4R mRNA after axotomy

We then examined the MC4R mRNA expression profile in the hypoglossal nucleus during the regeneration process from 1 day until 56 days after injury. The density of the hybridization signal in the hypoglossal nucleus on film was measured and the relative optical density unit was calculated. The increase in MC4R mRNA was significant from 3 to 7 days after nerve injury, decreasing to the control level by day 14 after injury (Fig. 3).

MC4R mRNA expression is induced in primary sensory neurons after axotomy

We next examined MC4R mRNA expression in axotomized primary sensory neurons. We extracted bilateral L4-6 DRGs 5 days after left sciatic nerve injury and performed RT-PCR with specific primers for all five MCR mRNAs (Fig. 4). The mRNAs for MC1R, MC2R, MC3R, and MC4R were faintly expressed in the control DRG, whereas MC5R mRNA was not detected. After nerve injury, MC1R mRNA expression did not change, the mRNA expression for MC2R and MC3R decreased, and MC4R mRNA expression increased. MC5R mRNA was not detected even after axotomy. These results demonstrate that MC4R mRNA expression is exclusively induced among the MCR family, and the induction of MC4R mRNA in response to axotomy seems to be a common phenomenon in peripheral sensory and motor neurons. We also performed *in situ* hybridization to identify MCR-positive neuron types in the DRG; however, clear accumulation of silver grain, which indicates an mRNA-positive signal, was not observed. This was probably because the amount of mRNA in DRG neurons was less than that in motor neurons, whereas

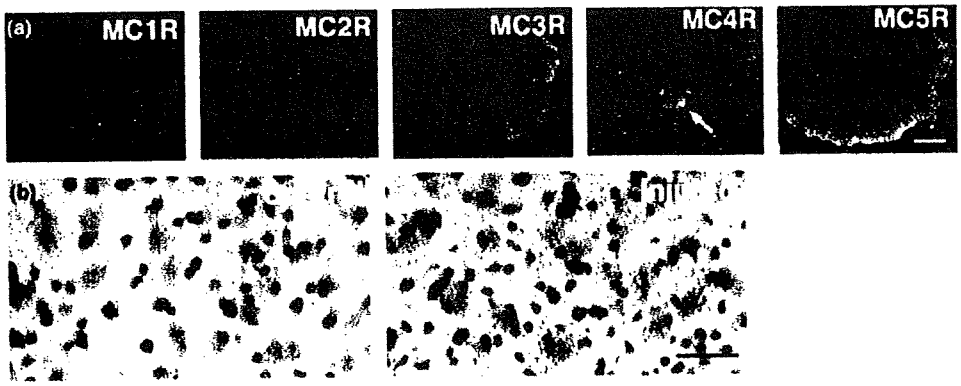

Fig. 2 (a) *In situ* hybridization study of the melanocortin receptor family on coronal brain sections, 5 days after the right hypoglossal nerve injury (right side). Melanocortin receptor (MCR) MC1R, MC2R, MC3R, and MC5R were not expressed in hypoglossal nuclei, either before or after axonal injury. By contrast, MC4R expression was seen at a low level in the intact hypoglossal nucleus and was increased after axonal injury. Scale bar: 1 mm. (b) Bright-field micrograph stained with thionin showing the localization of MC4R mRNA in the control and axotomized hypoglossal nuclei 5 days after the operation. There was a high density of grains localized mainly in large neurons on the injured side. Scale bar: 50 μm.

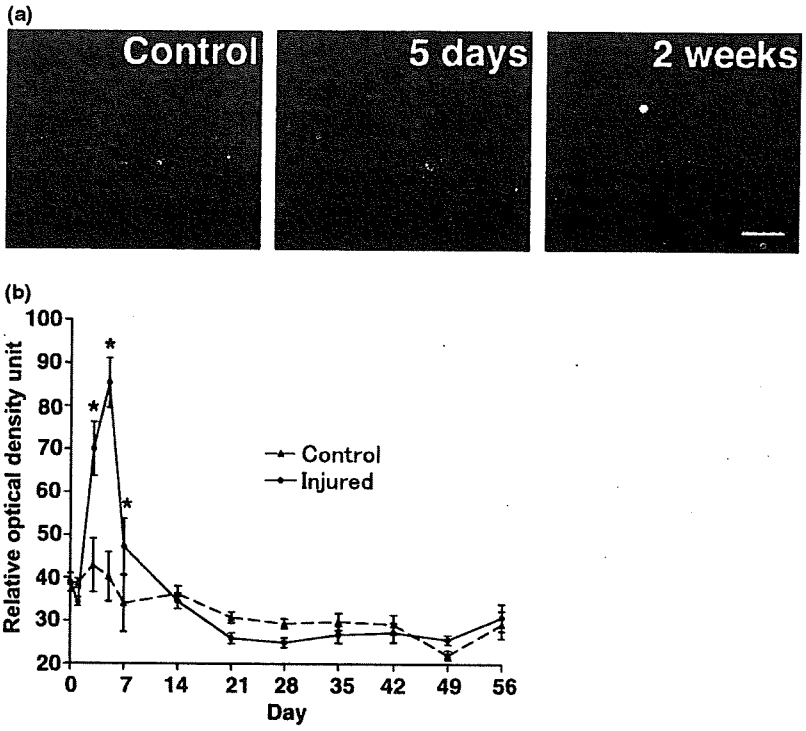

Fig. 3 *In situ* hybridization study of melanocortin receptor (MCR) MC4R in the hypoglossal nucleus from 0 to 56 days after axonal injury. (a) MC4R expression significantly increased on post-operative day 3, reached a peak on day 5, and decreased to the control level on day 14. Scale bar: 50 μm. (b) The signal density in nuclei was quantified and is shown as a graph. Data are means ± SEM from three independent experiments. *Asterisk* indicates statistically significant differences (Student's *t*-test) from control ($p < 0.05$).

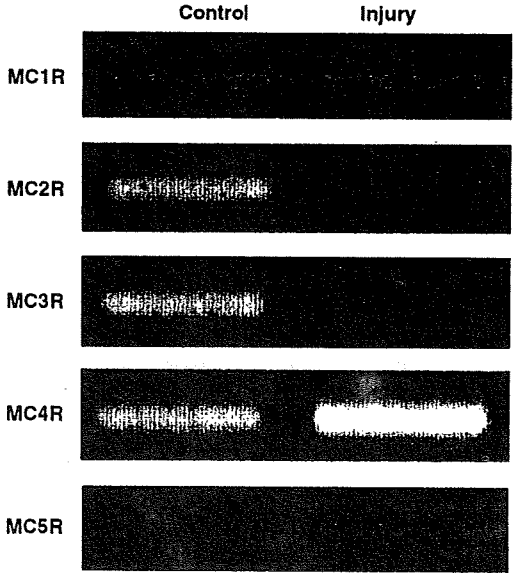

Fig. 4 RT-PCR study of the melanocortin receptor family in the L4-6 dorsal root ganglions (DRGs), 5 days after sciatic nerve injury. Expression of melanocortin receptor (MCR) MC1R, MC2R, and MC3R mRNAs was seen in intact DRGs. After sciatic nerve injury, MC1R expression did not change and the expression of MC2R and MC3R decreased. MC5R expression was not seen on either side. By contrast, MC4R mRNA was detected in intact DRGs and increased after axonal injury.

PCR could detect the existence and the alteration of mRNA expression in DRG.

Alpha-MSH promotes neurite outgrowth in cultured DRG neurons

We next examined whether alpha-MSH promotes neurite elongation in cultured mouse DRG neurons, because alpha-MSH is a potent ligand for MC4R. We cultured DRG neurons in media with four different concentrations (10^{-9}, 10^{-8}, 10^{-7}, and 10^{-6} mol/L) of alpha-MSH or 100 ng/mL nerve growth factor for 20 h and measured the length of the longest neurite on each neuron, according to the previously published method (Bonilla *et al.* 2002). Alpha-MSH significantly stimulated neurite outgrowth at a concentration of 10^{-8} mol/L (Fig. 5). The neurite elongation activity of alpha-MSH was comparable with that of nerve growth factor.

A selective MCR-4 antagonist suppresses neurite elongation induced by alpha-MSH

We then applied JKC-363, a selective MC4R antagonist, to cultured DRG neurons. JKC-363 has a 90-fold higher affinity for MC4R than for MC3R and blocks the cardiovascular and sympathetic responses to alpha-MSH (Kim *et al.* 2002; Matsumura *et al.* 2002). The application of 10^{-6} mol/L JKC-363 alone had no effect on the neurite length; however, JKC-363 completely blocked the effect of alpha-MSH when it was added simultaneously with alpha-MSH (Fig. 6). This result

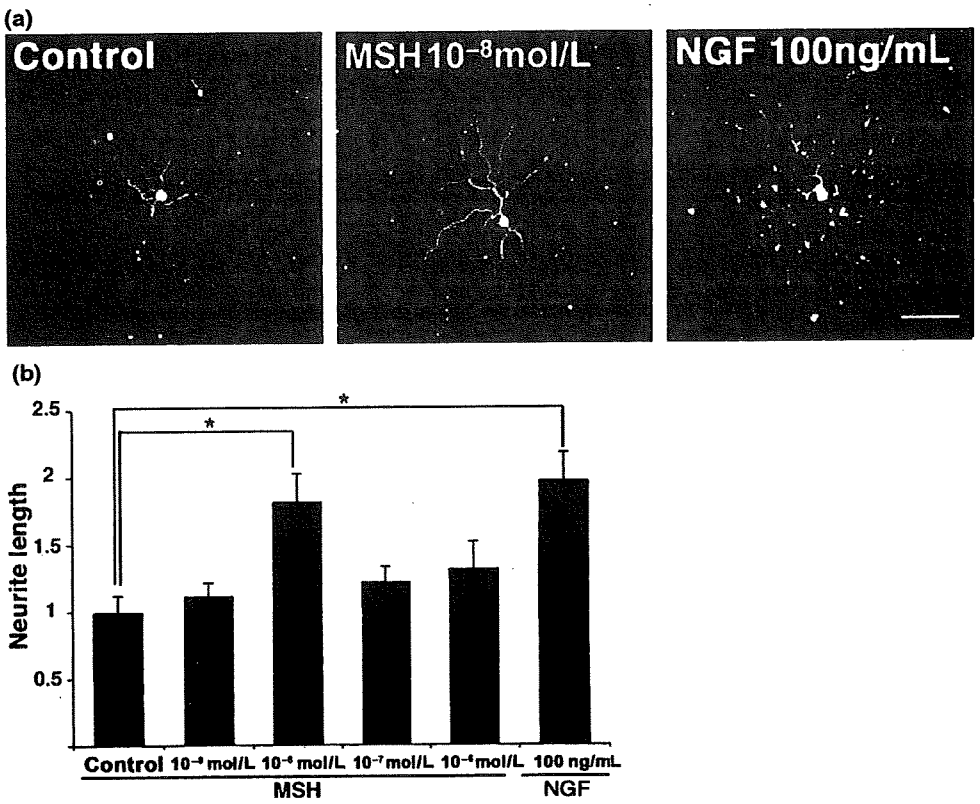

Fig. 5 Alpha-melanocortin stimulating hormone (MSH) stimulates neurite outgrowth in dorsal root ganglion neuron culture. Alpha-MSH at different concentrations was added to the culture media and neurite length was evaluated 20 h after cell spreading. (a) Neurites are visualized with anti-beta-tublin III antibody staining. Scale bar: 100 μm. (b) Alpha-MSH significantly increased neurite length only at a concentration of 10^{-8} mol/L. This effect was similar to that of 100 ng/mL nerve growth factor (NGF). Data are means ± SEM from three independent experiments. *Asterisk* indicates statistically significant differences (Student's *t*-test) from control ($p < 0.05$).

indicates that alpha-MSH could stimulate neurite elongation via MC4R.

Discussion

The present study demonstrates the prominent induction of MC4R mRNA in motor and primary sensory neurons in mice after axonal injury. In addition, we show that alpha-MSH could promote axonal outgrowth via MC4R in adult mouse DRG neurons and, perhaps, also in hypoglossal motor neurons.

Alpha-MSH and other ACTH analogs stimulate neurite outgrowth of several types of neurons (Van der Neut *et al.* 1988; van der Neut *et al.* 1992; Peulve *et al.* 1994; Adan *et al.* 1996; Joosten *et al.* 1996). Van der Neut *et al.* quantified neuritogenesis using ELISA for neurofilament protein in neonatal rat DRG neuron culture and reported that alpha-MSH stimulates neuritogenesis in a bell-shaped dose-responsive manner with a maximal effect at 100 nmol/L (van der Neut *et al.* 1992). In Neuro2A cells, alpha-MSH stimulates neurite outgrowth in the same dose-responsive manner and this effect is inhibited by the MC4R antagonist [D-Arg^8]ACTH(4–10) (Adan *et al.* 1996). Alpha-MSH is also capable of promoting the recovery of sensory and motor function in animals after sciatic nerve injury (Bijlsma *et al.* 1983; Verhaagen *et al.* 1986; Dekker 1988). Our *in vitro* result using adult mouse DRG neurons is consistent with those of previous studies. Although alpha-MSH administration promotes nerve regeneration, the source of endogenous alpha-MSH in peripheral nervous system has not yet been elucidated. The most likely source of alpha-MSH is the pituitary gland; indeed, the synthesis and release of melanocortins is induced in the pituitary gland in response to stress stimuli (Carr *et al.* 1990; Lindley *et al.* 1990; Lookingland *et al.* 1991). Therefore, alpha-MSH might be released into the circulation in response to the stress stimuli induced by nerve injury. Some reports described the possible existence of alpha-MSH-like peptides in degenerating nerves and DRG (Plantinga *et al.* 1992, 1995), whereas another report suggested that rat peripheral nerves contain no detectable alpha-MSH (Verhaagen *et al.* 1988). Although the source of endogenous melanocortin is unclear, the up-regulation of

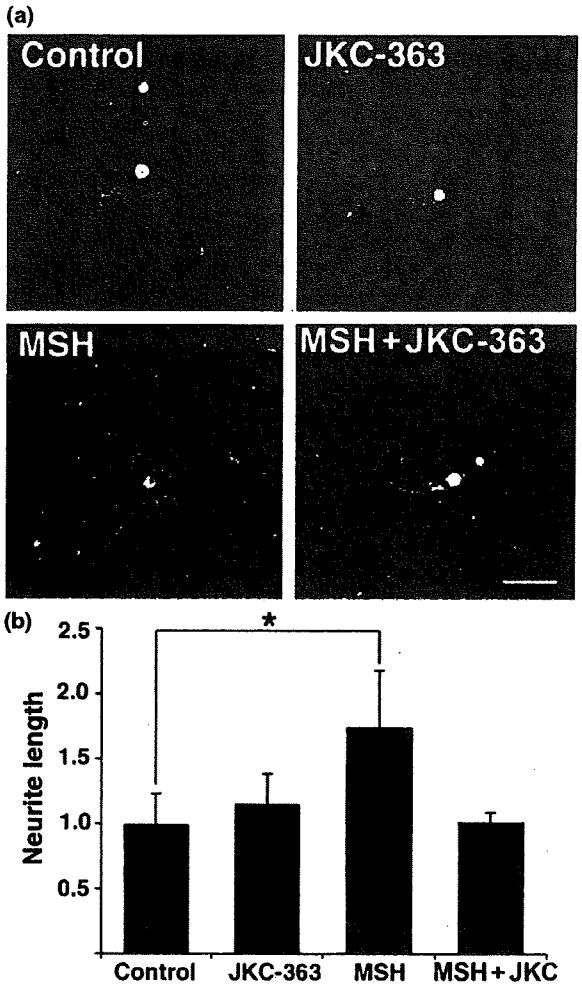

Fig. 6 A selective melanocortin receptor (MCR) MC4R antagonist, JKC-363, completely blocks neurite elongation induced by alpha-melanocortin stimulating hormone (MSH). Dorsal root ganglion neurons were cultured with 10^{-8} mol/L alpha-MSH and/or 10^{-6} mol/L JKC-363 and neurite length was measured 20 h after cell spreading. (a) Neurites are visualized with anti-beta-tublin III antibody staining. Scale bar: 100 μm. (b) Although 10^{-8} mol/L alpha-MSH significantly increased neurite length, this increase was inhibited by simultaneous addition of JKC-363. The application of 10^{-6} mol/L JKC-363 alone had no effect on neurite length. Data are means ± SEM from three independent experiments. *Asterisk* indicates statistically significant differences (Student's *t*-test) from control ($p < 0.05$).

MC4R expression in axotomized neurons is a feasible response and is, perhaps, a crucial event for endogenous melanocortins to support nerve regeneration.

From pharmacological aspects, two studies using several ACTH analogs speculate that MC4R is not involved in functional recovery after peripheral nerve injury (Adan *et al.* 1994); (Nijenhuis *et al.* 2004). In rats with sciatic nerve crush injury, administration of alpha-MSH, [N-Leu4, D-phe7]-alpha-MSH, ACTH4–10, or ORG2766 (ACTH4–9 analog) facilitates recovery of sensory-motor function, whereas gamma-MSH or [D-Phe^7]ACTH4–10 does not (Bijlsma *et al.* 1983) (Van der Zee *et al.* 1991). Adan *et al.* showed that ACTH4–10 has very low activity via MC4R that ORG2766 does not activate MC4R and that [D-Phe^7]ACTH4–10 is a much more potent activator of MC4R than ACTH4–10; this group also suggested that an MCR other than MC4R mediates functional recovery induced by alpha-MSH (Adan *et al.* 1994). Furthermore, because gamma-MSH is a potent activator of MC3R, they suggested that neither MC3R nor MC4R is involved in this effect of alpha-MSH. According to another report using several MSH analogs, functional recovery is not facilitated by an agonist of MC1/4R and is not inhibited by a MC3/4R antagonist (Nijenhuis *et al.* 2004). Their study concluded that MC5R might mediate nerve regeneration. Conflicting with these pharmacological observations in rats, the present study shows that expression of neither MC1R nor MC5R is detected in axotomized motor neurons of mouse, suggesting that they are not likely to function after peripheral nerve damage. By contrast, MC4R is strongly induced by peripheral nerve damage in mouse. We could not explain the reasons for the inconsistency between our study and the previous pharmacological reports; however, one possible explanation might be species difference. Axotomy induces slowly progressive motor neuron death in the adult mouse, but not in the adult rat. We previously demonstrated that some genes are oppositely regulated between rat and mouse and this difference sometimes leads to the different susceptibility of injured motor neurons (Kiryu-Seo *et al.* 2005) (Kiryu-Seo *et al.* 2006). For example, Noxa is induced in axotomized neurons of the adult mouse but not in the adult rat and mediates mouse motor neuron death after nerve injury. On the other hand, excitatory amino-acid carrier 1 is induced in axotomized neurons of the adult rat and down-regulated in the adult mouse, and is critical for motor neuron survival after nerve injury. In fact, our preliminary experiment using nerve-injured hypoglossal nucleus of rat did not show up-regulation of MC4R (data not shown). In any event, our present study suggests that MC4R is the most conceivable mediator for nerve regeneration, at least in mouse.

There were other controversial observations on the alteration of MC4R mRNA expression in cranial motor and primary sensory neurons in the previous reports. One report, using an RNase protection assay, demonstrated that a small amount of MC4R mRNA is expressed in the rat L4-6 spinal cord, but the expression level is not altered by sciatic nerve injury (van der Kraan *et al.* 1999). They did not detect any expression of MC4R in L4-6 DRGs, either before or after sciatic nerve injury. However, another study using RT-PCR reported that MC4R mRNA is expressed in rat DRGs (Starowicz *et al.* 2004). The MC4R mRNA level in DRGs was down-regulated in a rat neuropathic pain model (chronic

constriction injury model), but this alteration was not observed in the rat spinal cord (Starowicz *et al.* 2004). Confusingly, Vrinten *et al.* (2000) used an *in situ* ^{125}I-[N-Leu4, D-phe7]-alpha-MSH (a synthetic alpha-MSH analog) binding assay in chronic constriction injury rats and found that the MCR level in laminae I–II of the spinal cord at level L4-6, on both ipsilateral and contralateral sides to the injured nerve, was significantly higher in comparison with sham-operated animals. The present study clearly demonstrates the predominant expression of MC4R mRNA, among the MCR family, in mouse hypoglossal motor neurons and DRGs. In addition, MC4R mRNA expression was apparently up-regulated in response to axonal injury, while the expression level of the other MCRs mRNAs was not altered or even down-regulated. Again the discrepancy between other reports and the present study might be due to species differences (Kiryu-Seo *et al.* 2005, 2006). Our present results imply that MC4R is the principal mediator of melanocortin signaling in mouse motor and primary neurons during nerve regeneration. The melanocortins activate adenylate cyclase and thereby increase intracellular cAMP levels via their receptors (Gantz *et al.* 1993; Konda *et al.* 1994). The increase in cAMP could be a major reason why alpha-MSH facilitates neurite elongation. cAMP promotes neurite outgrowth in a variety of neuronal cell lines through the activation of protein kinase A (Snider *et al.* 2002). Therefore, it is suggested that during nerve regeneration, stimulation of MC4R promotes axonal outgrowth through an increase in cAMP. This MC4R-mediated signaling could have a synergistic effect on injured neurons together with other crucial growth factors such as glial cell line-derived neurotrophic factor and leukemia inhibitory factor, which induce major survival signaling pathways such as the Akt and STAT signaling pathways (Namikawa *et al.* 2000; Honma *et al.* 2002).

Acknowledgements

We are grateful to C Kadono, T Ogawa, and I Jikihara for their excellent technical assistance and T Kawai for secretarial assistance. This work was supported by grants from Ministry of Health, Labor and Welfare of Japan, MEXT, the General Insurance Association of Japan and Osaka City University Medical Research Foundation.

References

Adan R. A., Cone R. D., Burbach J. P. and Gispen W. H. (1994) Differential effects of melanocortin peptides on neural melanocortin receptors. *Mol. Pharmacol.* **46**, 1182–1190.

Adan R. A., van der Kraan M., Doornbos R. P., Bar P. R., Burbach J. P. and Gispen W. H. (1996) Melanocortin receptors mediate alpha-MSH-induced stimulation of neurite outgrowth in neuro 2A cells. *Brain Res. Mol. Brain Res.* **36**, 37–44.

Bijlsma W. A., Schotman P., Jennekens F. G., Gispen W. H. and De Wied D. (1983) The enhanced recovery of sensorimotor function in rats is related to the melanotropic moiety of ACTH/MSH neuropeptides. *Eur. J. Pharmacol.* **92**, 231–236.

Bonilla I. E., Tanabe K. and Strittmatter S. M. (2002) Small proline-rich repeat protein 1A is expressed by axotomized neurons and promotes axonal outgrowth. *J. Neurosci.* **22**, 1303–1315.

Carr J. A., Saland L. C., Samora A., Desai S. and Benevidez S. (1990) Stress-induced peptide release from rat intermediate pituitary. An ultrastructural analysis. *Cell Tissue Res.* **261**, 589–593.

Dekker A. J. (1988) Effect of alpha-melanocyte-stimulating hormone on peripheral nerve regeneration in the rat: histological aspects and comparison with the effect of gangliosides. *Exp. Neurol.* **99**, 490–497.

Gantz I., Miwa H., Konda Y., Shimoto Y., Tashiro T., Watson S. J., DelValle J. and Yamada T. (1993) Molecular cloning, expression, and gene localization of a fourth melanocortin receptor. *J. Biol. Chem.* **268**, 15174–15179.

Honma M., Namikawa K., Mansur K., Iwata T., Mori N., Iizuka H. and Kiyama H. (2002) Developmental alteration of nerve injury induced glial cell line-derived neurotrophic factor (GDNF) receptor expression is crucial for the determination of injured motoneuron fate. *J. Neurochem.* **82**, 961–975.

Joosten E. A., Verhaagh S., Martin D., Robe P., Franzen R., Hooiveld M., Doornbos R., Bar P. R. and Moonen G. (1996) Alpha-MSH stimulates neurite outgrowth of neonatal rat corticospinal neurons *in vitro*. *Brain Res.* **736**, 91–98.

Kim M. S., Small C. J., Russell S. H., Morgan D. G., Abbott C. R., alAhmed S. H., Hay D. L., Ghatei M. A., Smith D. M. and Bloom S. R. (2002) Effects of melanocortin receptor ligands on thyrotropin-releasing hormone release: evidence for the differential roles of melanocortin 3 and 4 receptors. *J. Neuroendocrinol.* **14**, 276–282.

Kiryu S., Yao G. L., Morita N., Kato H. and Kiyama H. (1995) Nerve injury enhances rat neuronal glutamate transporter expression: identification by differential display PCR. *J. Neurosci.* **15**, 7872–7878.

Kiryu-Seo S., Hirayama T., Kato R. and Kiyama H. (2005) Noxa is a critical mediator of p53-dependent motor neuron death after nerve injury in adult mouse. *J. Neurosci.* **25**, 1442–1447.

Kiryu-Seo S., Gamo K., Tachibana T., Tanaka K. and Kiyama H. (2006) Unique anti-apoptotic activity of EAAC1 in injured motor neurons. *EMBO J.* **25**, 3411–3421 (Epub Jul 2006 3413).

Konda Y., Gantz I., DelValle J., Shimoto Y., Miwa H. and Yamada T. (1994) Interaction of dual intracellular signaling pathways activated by the melanocortin-3 receptor. *J. Biol. Chem.* **269**, 13162–13166.

Konishi H., Namikawa K. and Kiyama H. (2006) Annexin III implicated in the microglial response to motor nerve injury. *Glia* **53**, 723–732.

Lankhorst A. J., Duis S. E., ter Laak M. P., Joosten E. A., Hamers F. P. and Gispen W. H. (1999) Functional recovery after central infusion of alpha-melanocyte-stimulating hormone in rats with spinal cord contusion injury. *J. Neurotrauma* **16**, 323–331.

Lindley S. E., Lookingland K. J. and Moore K. E. (1990) Dopaminergic and beta-adrenergic receptor control of alpha-melanocyte-stimulating hormone secretion during stress. *Neuroendocrinology* **52**, 46–51.

Lookingland K. J., Gunnet J. W. and Moore K. E. (1991) Stress-induced secretion of alpha-melanocyte-stimulating hormone is accompanied by a decrease in the activity of tuberohypophysial dopaminergic neurons. *Neuroendocrinology* **53**, 91–96.

Matsumura K., Tsuchihashi T., Abe I. and Iida M. (2002) Central alpha-melanocyte-stimulating hormone acts at melanocortin-4 receptor to activate sympathetic nervous system in conscious rabbits. *Brain Res.* **948**, 145–148.

Namikawa K., Honma M., Abe K., Takeda M., Mansur K., Obata T., Miwa A., Okado H. and Kiyama H. (2000) Akt/protein kinase B prevents injury-induced motoneuron death and accelerates axonal regeneration. *J. Neurosci.* **20**, 2875–2886.

Nijenhuis W. A., Wanders N., Kruijtzer J. A., Liskamp R. M., Gispen W. H. and Adan R. A. (2004) Accelerating sensory recovery after sciatic nerve crush: non-selective versus melanocortin MC4 receptor-selective peptides. *Eur. J. Pharmacol.* **495**, 145–152.

Peulve P., Laquerriere A., Hemet J. and Tadie M. (1994) Comparative effect of alpha-MSH and b-FGF on neurite extension of fetal rat spinal cord neurons in culture. *Brain Res* **654**, 319–323.

Plantinga L. C., Verhaagen J., Edwards P. M., Schrama L. H., Burbach J. P. and Gispen W. H. (1992) Expression of the pro-opiomelanocortin gene in dorsal root ganglia, spinal cord and sciatic nerve after sciatic nerve crush in the rat. *Brain Res. Mol. Brain Res.* **16**, 135–142.

Plantinga L. C., Verhaagen J., Edwards P. M., Hali M., Brakkee J. H. and Gispen W. H. (1995) Pharmacological evidence for the involvement of endogenous alpha-MSH-like peptides in peripheral nerve regeneration. *Peptides* **16**, 319–324.

Snider W. D., Zhou F. Q., Zhong J. and Markus A. (2002) Signaling the pathway to regeneration. *Neuron* **35**, 13–16.

Starowicz K. and Przewlocka B. (2003) The role of melanocortins and their receptors in inflammatory processes, nerve regeneration and nociception. *Life Sci.* **73**, 823–847.

Starowicz K., Bilecki W., Sieja A., Przewlocka B. and Przewlocki R. (2004) Melanocortin 4 receptor is expressed in the dorsal root ganglions and down-regulated in neuropathic rats. *Neurosci. Lett.* **358**, 79–82.

Tanabe K., Kiryu-Seo S., Nakamura T., Mori N., Tsujino H., Ochi T. and Kiyama H. (1998) Alternative expression of Shc family members in nerve-injured motoneurons. *Brain Res. Mol. Brain Res.* **53**, 291–296.

Tanabe K., Nakagomi S., Kiryu-Seo S., Namikawa K., Imai Y., Ochi T., Tohyama M. and Kiyama H. (1999) Expressed-sequence-tag approach to identify differentially expressed genes following peripheral nerve axotomy. *Brain Res. Mol. Brain Res.* **64**, 34–40.

Tanabe K., Tachibana T., Yamashita T., Che Y. H., Yoneda Y., Ochi T., Tohyama M., Yoshikawa H. and Kiyama H. (2000) The small GTP-binding protein TC10 promotes nerve elongation in neuronal cells, and its expression is induced during nerve regeneration in rats. *J. Neurosci.* **20**, 4138–4144.

Tanabe K., Bonilla I., Winkles J. A. and Strittmatter S. M. (2003) Fibroblast growth factor-inducible-14 is induced in axotomized neurons and promotes neurite outgrowth. *J. Neurosci.* **23**, 9675–9686.

Van der Kraan M., Tatro J. B., Entwistle M. L., Brakkee J. H., Burbach J. P., Adan R. A. and Gispen W. H. (1999) Expression of melanocortin receptors and pro-opiomelanocortin in the rat spinal cord in relation to neurotrophic effects of melanocortins. *Brain Res. Mol. Brain Res.* **63**, 276–286.

Van der Neut R., Bar P. R., Sodaar P. and Gispen W. H. (1988) Trophic influences of alpha-MSH and ACTH4-10 on neuronal outgrowth *in vitro*. *Peptides* **9**, 1015–1020.

Van der Neut R., Hol E. M., Gispen W. H. and Bar P. R. (1992) Stimulation by melanocortins of neurite outgrowth from spinal and sensory neurons *in vitro*. *Peptides* **13**, 1109–1115.

Van der Zee C. E., Brakkee J. H. and Gispen W. H. (1991) Putative neurotrophic factors and functional recovery from peripheral nerve damage in the rat. *Br. J. Pharmacol.* **103**, 1041–1046.

Verhaagen J., Edwards P. M., Jennekens F. G., Schotman P. and Gispen W. H. (1986) Alpha-melanocyte-stimulating hormone stimulates the outgrowth of myelinated nerve fibers after peripheral nerve crush. *Exp. Neurol.* **92**, 451–454.

Verhaagen J., Edwards P. M. and Gispen W. H. (1988) Damaged rat peripheral nerves do not contain detectable amounts of alpha-MSH. *J. Neurosci. Res.* **19**, 14–18.

Vrinten D. H., Gispen W. H., Groen G. J. and Adan R. A. (2000) Antagonism of the melanocortin system reduces cold and mechanical allodynia in mononeuropathic rats. *J. Neurosci.* **20**, 8131–8137.

Available online at www.sciencedirect.com
ScienceDirect
Behavioural Brain Research 180 (2007) 69–76
BEHAVIOURAL BRAIN RESEARCH
www.elsevier.com/locate/bbr

Research report

Enriched environments influence depression-related behavior in adult mice and the survival of newborn cells in their hippocampi

Satoko Hattori [a], Ryota Hashimoto [a,b,c,*], Tsuyoshi Miyakawa [d], Hajime Yamanaka [a], Hiroshi Maeno [e], Keiji Wada [e], Hiroshi Kunugi [a]

[a] *Department of Mental Disorder Research, National Institute of Neuroscience, National Center of Neurology and Psychiatry, 4-1-1 Ogawahigashi, Kodaira, Tokyo 187-8502, Japan*
[b] *The Osaka-Hamamatsu Joint Research Center for Child Mental Development, Osaka University Graduate School of Medicine, 2-2 Yamadaoka, Suita, Osaka 565-0871, Japan*
[c] *Department of Psychiatry, Osaka University Graduate School of Medicine, 2-2 Yamadaoka, Suita, Osaka 565-0871, Japan*
[d] *Horizontal Medical Research Organization, Kyoto University Faculty of Medicine, Yoshida-Konoe, Sakyo-ku, Kyoto 606-8501, Japan*
[e] *Department of Degenerative Neurological Disease, National Institute of Neuroscience, National Center of Neurology and Psychiatry, 4-1-1 Ogawahigashi, Kodaira, Tokyo 187-8502, Japan*

Received 1 September 2006; received in revised form 14 February 2007; accepted 20 February 2007
Available online 28 February 2007

Available online at www.sciencedirect.com
ScienceDirect
Behavioural Brain Research 180 (2007) 69–76
BEHAVIOURAL BRAIN RESEARCH
www.elsevier.com/locate/bbr

Research report

Enriched environments influence depression-related behavior in adult mice and the survival of newborn cells in their hippocampi

Satoko Hattori [a], Ryota Hashimoto [a,b,c,*], Tsuyoshi Miyakawa [d], Hajime Yamanaka [a], Hiroshi Maeno [e], Keiji Wada [e], Hiroshi Kunugi [a]

[a] *Department of Mental Disorder Research, National Institute of Neuroscience, National Center of Neurology and Psychiatry, 4-1-1 Ogawahigashi, Kodaira, Tokyo 187-8502, Japan*
[b] *The Osaka-Hamamatsu Joint Research Center for Child Mental Development, Osaka University Graduate School of Medicine, 2-2 Yamadaoka, Suita, Osaka 565-0871, Japan*
[c] *Department of Psychiatry, Osaka University Graduate School of Medicine, 2-2 Yamadaoka, Suita, Osaka 565-0871, Japan*
[d] *Horizontal Medical Research Organization, Kyoto University Faculty of Medicine, Yoshida-Konoe, Sakyo-ku, Kyoto 606-8501, Japan*
[e] *Department of Degenerative Neurological Disease, National Institute of Neuroscience, National Center of Neurology and Psychiatry, 4-1-1 Ogawahigashi, Kodaira, Tokyo 187-8502, Japan*

Received 1 September 2006; received in revised form 14 February 2007; accepted 20 February 2007
Available online 28 February 2007

Abstract

Major depression is a highly prevalent mental disorder and environmental factors have been strongly implicated in its pathophysiology. Clinica studies have demonstrated that stress or depression can lead to atrophy and cell loss in the hippocampus. Studies of animal models of depressio have suggested that reduced neurogenesis in the adult hippocampus might contribute to such structural changes and to the behavior of thes animals. On the other hand, increased hippocampal neurogenesis can be induced by the administration of antidepressants or electroconvulsiv seizure, suggesting that increased neurogenesis might be related to the treatment of depression. Thus, an enriched environment (EE), which als enhances neurogenesis, is expected to have therapeutic effects on depression-related behaviors. To investigate the effects of an EE during adulthoo on these behaviors, we subjected adult mice housed in an EE for five weeks to behavioral tests. In an open field test, EE mice exhibited a decreas in the distance traveled and an increase in the amount of time spent in the center. The startle response was smaller in EE mice than in control mice EE mice also showed reduced immobility time in a forced swim test. The immobility time in EE mice was approximately half that observed i mice treated with a tricyclic antidepressant, imipramine. In our experimental condition, increased survival of newborn cells was observed in El mice by 5-bromo-2′-deoxyuridine (BrdU)-labeled immunohistochemistry. Double-staining of BrdU and a mature neuron marker, NeuN, reveale that the majority of surviving cells were neurons. Our results suggest that EE, which enhanced the survival of newborn neurons, shows benefici effects on behavioral despair and habituation to a novel environment.

Keywords: Enriched environment; Depression; Antidepressant; BrdU; Forced swim test; Neurogenesis

1. Introduction

Major depressive disorder is a common mental disease with a lifetime prevalence of ~20% [41]. Although genetic susceptibility has been considered to be involved in the disorder, sever stressors have also been associated with a substantial increas in its risk [22,26]. In rodents, models of depression rely o responses to stress, and show particular aspects of the disorde for example, cognitive or attentional impairment and abnormal ties in psychomotor activity [9,32]. Moreover, stressors produc dendritic atrophy, death or endangerment of hippocampal neu rons [27], and inhibit neurogenesis in the adult hippocampu [12,15]. This evidence suggests that stress-induced structur and/or functional alterations in the hippocampus have importa

* Corresponding author at: The Osaka-Hamamatsu Joint Research Center for Child Mental Development, Osaka University Graduate School of Medicine, 2-2 Yamadaoka, Suita, Osaka 565-0871, Japan. Tel.: +81 6 6879 3074; fax: +81 6 6879 3059.
E-mail address: hashimor@psy.med.osaka-u.ac.jp (R. Hashimoto).

0166-4328/$ – see front matter © 2007 Elsevier B.V. All rights reserved.
doi:10.1016/j.bbr.2007.02.036

roles in the pathogenesis of depression. Indeed, brain imaging studies have reported that hippocampal volume is decreased in patients with depression [3,36].

Recent studies have reported that neurons are produced in the hippocampus throughout the lifetime of animals, including humans [13]. The number of new granule neurons generated each month is 6% of the total granule cell population [5]. The axons of adult-generated hippocampal neurons extend into the CA3 region [18,39], and newborn cells mature into functional neurons in the hippocampus [39]. A substantial reduction in the number of newly generated cells impairs hippocampal-dependent forms of associative memory formation [37]. Moreover, adult hippocampal neurogenesis is enhanced by the administration of electroconvulsive seizure [23,25] or antidepressant treatment [25,35]. These findings indicate that adult-generated neurons may contribute in a significant manner to the functions of the hippocampus, and that increased neurogenesis may underlie the therapeutic effects of treatments for depression.

Enriched environments (EEs) also increase the number of new neurons in the adult dentate gyrus [20], and reduce spontaneous apoptotic cell death in the hippocampus [42]. It has been reported that EEs modify hippocampal functions such as long-term potentiation, through cAMP-dependent protein kinase [11], and hippocampus-dependent memory [4,11,20]. These findings suggest that environmental enrichment is also expected to have effects on depression-related behaviors. A preweaning EE paradigm is known to reduce the immobility time in a forced swim test [24], a variable that is considered to reflect "behavioral despair" [34]. However, the effects of environmental enrichment during adulthood are poorly understood. Thus, we performed a behavioral analysis of adult mice housed in an EE.

2. Materials and methods

2.1. Animals

Inbred C57BL/6J female mice were used in this study and were housed in a temperature-controlled room under a 12 h light–dark cycle (light on at 8:00 a.m.) with ad libitum access to food and water. The control condition consisted of three mice in a common cage housing (190 mm × 260 mm × 125 mm). The EE condition consisted of three mice in a large rodent cage (350 mm × 400 mm × 180 mm) containing three toys – a running wheel, plastic tube and wooden swing – in addition to several wooden environmental enrichment products (Tapvei Oy, Kortteinen, Finland), which were changed once per week. For each experiment, we used the batches of mice, which were housed in each condition from 10 weeks of age. The experimental protocols were approved by the Ethics Review Committee for Animal Experimentation of the National Institute of Neuroscience, Japan.

2.2. Experimental design for behavioral tests

Behavioral tests were carried out with mice that had been housed in the control or EE condition for five weeks at start of testing (15 weeks old). Mice were maintained in their housing condition throughout all tests. All behavioral tests were performed between 9:00 a.m. and 7:00 p.m.. We prepared seven independent batches of mice for behavioral tests ($n=234$); one batch consisted of the same number of EE and control mice (EE: $n=9$ or 18, control: $n=9$ or 18). Neurological tests (in five batches), wire hang tests (in five batches), open field tests (in four batches), elevated plus maze tests (in three batches), social interaction tests (in three batches), startle response/prepulse inhibition tests (in two batches), and forced swim tests (no treat: in two batches; imipramine treat: in three batches), were conducted. The variances in the data among the batches were analyzed statistically (see Section 2.12). To minimize carryover effects of experimental manipulation on behavior, at least one day of rest was allotted between tests.

2.3. Neurological/motor function tests

The righting, whisker twitch, eye blink and ear twitch reflexes were evaluated. A number of physical features, including the presence of whiskers and bald patches, were also recorded.

Neuromuscular strength and balance were examined with the wire hang test. A mouse was placed on a wire cage lid, and then the lid was inverted and held at a height of approximately 30 cm above the cage litter. Latency to fall onto the bedding was recorded, with a 60 s cutoff time.

2.4. Open field test

Locomotor activity was measured using an open field test. It was recorded during the first exposure to the open field apparatus (50 cm × 50 cm × 40 cm; O'hara & Co., Tokyo, Japan). The illumination level was 22 lx at the floor of the open field. The apparatus was cleaned with water after each trial. The field was divided by software (see below) into 16 equal-sized squares containing 4 central areas and 12 peripheral areas. Horizontal activity, time spent in the central area and the number of fecal boli were recorded. Data were collected for 30 min. Data acquisition and analysis were performed automatically, using Image OF software (see Section 2.9).

2.5. Startle response/prepulse inhibition test

Response to acoustic startle and prepulse inhibition (PPI) of the startle response were measured using a startle reflex measurement system (O'hara & Co., Tokyo, Japan). A test session began by placing a mouse in a Plexiglas cylinder and leaving the mouse undisturbed for 10 min. The cylinder was cleaned with water after each trial. The startle stimulus was white noise for 20 ms at 110 or 120 dB, and the background noise level was 70 dB. The prepulse sound was presented 100 ms before the startle stimulus, for 20 ms, and its intensity was 74 or 78 dB. Four combinations of prepulse and startle stimuli were used (74/110, 78/110, 74/120 and 78/120 dB). Six blocks of six different trial types (four trial types with the combinations of prepulse and startle stimulus and two startle stimulus only trials) were presented in a pseudorandom order such that each trial type was presented once within a block. The average intertrial interval was 15 s (range, 10–20 s). The startle response was recorded for 500 ms starting with the onset of the startle stimulus, and the maximum startle amplitude (I_{max}) was determined. After the test, average values of I_{max} were calculated for the six trial types. The %PPI was defined as $[\{I_{max}\text{ (startle stimulus)}\} - \{I_{max}\text{ (prepulse and startle stimulus)}\}]/I_{max}\text{ (startle stimulus)} \times 100$.

2.6. Social interaction test

A pair of mice was placed simultaneously at opposing corners in the open field apparatus (50 cm × 50 cm × 40 cm; O'hara & Co., Tokyo, Japan) and allowed to explore freely for 10 min. We performed a social interaction test in a familiar situation with dim light [14]. The pair of mice had been housed in same environment condition but different cages. The illumination level was 22 lx at the floor of the open field. Mice were familiar with the apparatus because they had previously performed the open field test for 30 min in the same apparatus. The apparatus was cleaned with water after each trial. Total duration of contacts, number of contacts and total distance traveled were measured. Analysis was performed automatically using Image SI software (see Section 2.9).

2.7. Elevated plus maze test

The elevated plus maze consisted of two open arms (25 cm × 5 cm) with 3-mm-high ledges and two enclosed arms of the same size, with 15-cm-high transparent walls (O'hara & Co., Tokyo, Japan). The arms and central square

were made of white plastic and were elevated to a height of 34 cm above the floor. Arms of the same type were arranged at opposite sides to each other. A mouse was placed in the central square of the maze (5 cm × 5 cm), facing one of the enclosed arms. Behavior was recorded during a 10 min test session. The illumination level was 40 lx at the central square of the maze. The maze was cleaned with water after each trial. For data analysis, we used the following three measures: the percentage of time spent in the open arms, the percentage of open arm entries and the total number of arm entries. Data acquisition and analysis were performed automatically, using Image EP software (see Section 2.9).

2.8. Forced swim test

The apparatus consisted of a Plexiglas cylinder (22 cm height × 11.5 cm diameter). A modified forced swim test [8], in which the cylinder was filled with water (23–25 °C) up to a height of 17 cm, was used. A mouse was placed inside the cylinder, and the immobility time was recorded over a 10 min test period. The illumination level was 100 lx on the desk that the cylinder was placed on. Data acquisition and analysis were performed automatically, using Image FZ software (see Section 2.9). To estimate antidepressant-like effects of environmental enrichment, mice were administered intraperitoneally with imipramine, a tricyclic antidepressant (10 mg/kg; Sigma, St. Louis, MO) or saline, 30 min before the tests. We randomly divided the mice in a batch into four groups (EE + imipramine, EE + saline, control + imipramine and control + saline), and performed forced swim tests. Imipramine was dissolved in sterile saline.

2.9. Behavioral data analysis

Behavioral data from the open field tests, startle response/prepulse inhibition tests, social interaction tests, elevated plus maze tests and forced swim tests were automatically analyzed as described previously [29,30]. Briefly, behaviors were monitored by a color charged-coupled device camera (Watec Co., Ltd., Yamagata, Japan) that was connected to a Macintosh computer. Images were captured at one or two frames per second. All applications used for the behavioral studies (Image OF, Image EP, Image SI, Image FZ) were run using a Macintosh computer. These applications were based on the public domain NIH Image program (developed at the U.S. National Institute of Mental Health and available on the Internet at http://rsb.info.noh.gov/nih-image/) and were modified for each test by one of the authors (Tsuyoshi Miyakawa, available through O'hara & Co., Tokyo, Japan).

2.10. Immunohistochemistry

Mice were housed in a control or EE condition from 10 weeks of age, and injected with 5-bromo-2′-deoxyuridine (BrdU; Sigma, St. Louis, MO, 75 mg/kg, i.p.) at 15 weeks of age. BrdU is incorporated into DNA as bromouracil during the S phase of the cell cycle, to label newly generated cells. BrdU was dissolved in 0.9% NaCl and sterile-filtered at 0.2 μm. The solution was adjusted to a pH of 7.4 using 1N NaOH. Mice were maintained in their housing conditions until they were sacrificed at day one (proliferation paradigm) or four weeks (survival paradigm) after injection. Thirty mice (proliferation paradigm: $n = 18$; survival paradigm: $n = 12$) were used for histological analyses, and these were separate from the animals used for behavioral tests.

Mice were anaesthetized with sodium pentobarbital and transcardially perfused with 4% paraformaldehyde. Brains were removed, post-fixed in 4% paraformaldehyde overnight at 4 °C, and stored in a 30% sucrose solution. Coronal freezing microtome sections were stored in cryoprotectant (25% ethylene glycol, 25% glycerin, 0.05 M phosphate buffer, 0.01% sodium azide) at −20 °C until use.

Sections were immunostained as described previously with some modifications [16,17]. Free-floating sections were thoroughly rinsed with TBS (0.05 M Tris-base, 0.15 M NaCl adjusted to pH 7.4 using HCl). DNA was denatured by incubating sections in 2N HCl for 2 h at room temperature. Diaminobenzidine staining was performed with a monoclonal rat anti-BrdU antibody (1:200; Accurate Chemical & Scientific Corporation, Westbury, NY), an anti-rat biotinylated secondary antibody (1:200; Vector Laboratories, Inc., Burlingame, CA) and avidin-biotin-peroxidase complex (Vector Laboratories, Inc.). For double-immunofluorescence staining, combinations of the following primary antibodies were used: a monoclonal rat anti-BrdU antibody (1:200), a monoclonal mouse anti-neuronal nuclei (NeuN) antibody (1:200; Chemicon International, Inc., Temecula, CA) or a polyclonal rabbit anti-glial fibrillary acidic protein (GFAP) antibody (1:1000; Chemicon). Alexa 555 anti-rat, and Alexa 488 anti-rabbit or Alexa 488 anti-mouse (highly cross-adsorbed) IgG (H + L) (Molecular Probes, Inc., Eugene, OR) secondary antibodies (all generated in goat) were used.

2.11. Stereological analysis

Every sixth section was selected from serial coronal sections (40 μm) through the entire hippocampus of each animal and processed for immunostaining. Hippocampal sections were analyzed for immunopositive cells in the granule cell layer (GCL) and the subgranular zone (SGZ: within two cell body diameter from the edge of the GCL). The total number of BrdU-positive cells was determined in 9.9 ± 0.2 slices per mouse (not lower than eight slices). Cells were counted at 400-fold magnification using an optical microscope (Axiovert 200, Zeiss, Tokyo, Japan). The total number of BrdU-labeled cells in the dentate gyrus was estimated by multiplying the number of cells counted in every sixth section by six. For double-staining, slices were analyzed on a confocal laser-scanning microscope (Fluoview BX50; laser, Argon 488 nm and HeNe 543 nm; Olympus, Tokyo, Japan). At least 50 BrdU-labelled cells per animal were randomly selected from throughout the dentate gyrus and analyzed for the coexpression of BrdU and NeuN or GFAP. We measured GCL volume (EE: $n = 6$, control: $n = 6$) as described previously, with minor modifications [4,20]. Briefly, a one-in-six series of adjacent sections stained with Mayer's Hematoxylin solution (Wako Pure Chemical Industries Ltd., Osaka, Japan) for 3 min was used to trace the GCL area. The GCL images were captured with a 10-fold objective (Axiovert 200 controlled by Slide Book™ 3.0 (Intelligent Imaging Innovations, Inc., Denver, CO)). The stained GCL area was traced and the number of pixels within this area was automatically measured using Slide Book™ 3.0. The reference volume was estimated by summing the traced granule cell areas for each section multiplied by the distance between sections sampled (240 μm).

2.12. Statistical analysis

Statistical analysis was conducted using SPSS 11.0J for Windows (SPSS Japan, Inc., Tokyo, Japan). The variances in the data from different batches of mice were analyzed by two-way ANOVA. No significant batch-environmental interaction effect on behaviors was observed. Where significant batch effects on behavioral data (time spent in the center area in open field test, startle response, and total immobility time during the test in EE and control mice administered with imipramine or saline) were not found, we present total results for all of the batches. Where significant batch effects on behavioral data were observed, we show data from a representative batch analyzed by a two-tailed t test. Fisher's exact test was used to compare EE and control mice for general health (physical characteristics, sensory/motor reflexes and motor test). Time courses of distance traveled in the open field test and immobility time in the forced swim test were analyzed by repeated measures ANOVA. Values in the table and figures are expressed as means ± standard error of the mean (S.E.M.).

3. Results

3.1. General health in EE mice

An EE had no significant effect on either physical characteristics (whiskers and fur) or sensory-motor reflexes (eye blink, ear twitch, whisker response and righting reflex) (all p values >0.05) (Table 1). EE mice weighed 2% more than control mice ($p < 0.001$), and exhibited a longer latency to fall in the wire hang test ($p = 0.009$) (Table 1); however, there were no significant correlations between any of the measurements from the behavioral tests and weight or latency to fall (all p values >0.05).

Table 1
General physical characteristics and sensory/motor function in control and EE mice

	EE mice	Control mice	p value
Physical characteristics			
Weight (g)	22.0 ± 0.09	21.6 ± 0.09	<0.001
Whiskers (% with)	96.3	95.8	1.00
Fur (% with normal fur)	100	95.1	0.12
Sensory/motor reflex			
Eye blink (% with normal response)	95.1	97.5	0.68
Ear twitch (% with quick response)	97.5	100	0.50
Whisker twitch (% normal response)	93.6	88.2	0.19
Righting reflex (% normal response)	100	100	1.00
Motor test			
Wire hang (latency to fall; s)	60.0 ± 0.0	56.0 ± 1.3	0.009

Data represent the means ± S.E.M. (enriched environment, $n = 81$; control, $n = 81$).

3.2. Locomotor activity, anxiety and social behaviors in EE mice

We first examined the effect of an EE in the open field test (Fig. 1A and B). The distance traveled was shorter in EE mice (time course in Fig. 1A, environmental effect, $F(1,34) = 7.94$, $p = 0.008$; total distance during the test in Fig. 1B, $t(124) = 4.00$, $p < 0.001$). We then compared time spent in the center of the open field apparatus, between EE and control mice. EE mice spent significantly more time in the center than control mice did (Fig. 1C, $t(124) = 2.62$, $p = 0.010$). There was no significant

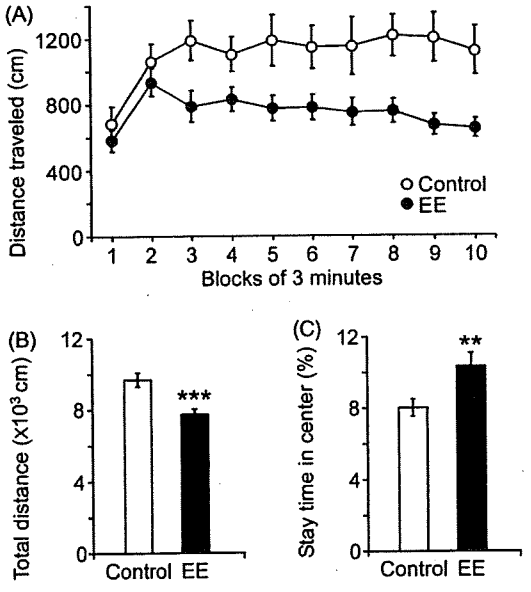

Fig. 1. Locomotor activity of EE mice in the open field test. (A) Time course of distance traveled. Representative data for four independent batches of mice are shown (EE: $n = 18$, control: $n = 18$). (B) Total distance traveled. (C) Time spent in the central area. Results from four batches of mice are shown in (B) and (C) (EE: $n = 63$, control: $n = 63$). Data represent means ± S.E.M. $^{**}p < 0.01$, $^{***}p < 0.001$.

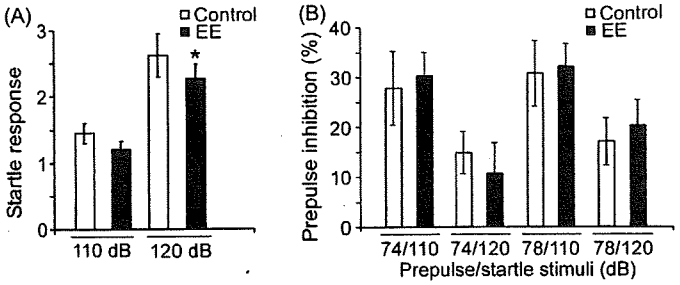

Fig. 2. Startle response and the prepulse inhibition in EE mice. (A) Startle response. Results from two batches of mice are shown (EE: $n = 36$, control: $n = 35$). (B) Prepulse inhibition of the startle response. Representative data for two independent batches of mice are shown (EE: $n = 18$, control: $n = 18$). Data represent means ± S.E.M. $^{*}p < 0.05$.

difference between EE and control mice in the number of fecal boli during the open field test (data not shown).

We also examined startle reactivity in EE mice. The response to 120 dB in EE mice was smaller than that in control mice (Fig. 2A, $t(69) = 2.17$, $p = 0.034$), and similar results were observed in the responses to 110 dB (Fig. 2A, $t(69) = 1.57$, $p = 0.12$). However, there was no significant difference in PPI between EE and control mice (Fig. 2B, 74/110 dB: $t(34) = 0.28$, $p = 0.78$, 78/110 dB: $t(34) = 0.57$, $p = 0.57$, 74/120 dB: $t(34) = 0.19$, $p = 0.85$, 78/120 dB: $t(34) = 0.47$, $p = 0.64$).

In the social interaction test, EE mice showed a significant decrease in the number of social contacts compared with control mice (Fig. 3A, $t(16) = 2.47$, $p = 0.034$); however, there was no significant difference in the total duration of contacts between EE and control mice (Fig. 3B, $t(16) = 1.79$, $p = 0.093$). Moreover, the total distance traveled was also less in EE mice (Fig. 3C, $t(16) = 3.18$, $p = 0.012$). The number and total duration of contacts per distance traveled did not differ significantly between EE and control mice (data not shown).

We then performed the elevated plus maze test. No significant differences between EE and control mice were found in the three parameters examined: the percentage of time spent in the open arms (Fig. 3D, $t(34) = 0.29$, $p = 0.78$), the percentage of open arm entries (Fig. 3E, $t(34) = 0.80$, $p = 0.43$) and the total number of arm entries (Fig. 3F, $t(34) = 0.42$, $p = 0.68$).

3.3. Depression-related behavior in EE mice

In this test, EE mice spent significantly less immobility time than control mice (time course in Fig. 4A, environmental effect, $F(1,52) = 8.75$, $p = 0.005$; total immobility time during the test in Fig. 4B, $t(52) = 2.96$, $p = 0.005$). As antidepressants are known to decrease immobility time [10,34], we compared the immobility times between EE mice and mice administered antidepressants. The time courses of immobility time for all cases of drug-treated mice, are shown in Fig. 4C. We confirmed that an EE reduced the total immobility time when treated with saline (Fig. 4D, $t(52) = 3.84$, $p < 0.001$). Control mice treated with imipramine showed a significant decrease in immobility compared with EE mice treated with saline (Fig. 4D, $t(52) = 2.69$, $p = 0.010$). The total immobility time was similar for EE and control mice after imipramine administration (Fig. 4D, $t(52) = 0.009$, $p = 0.993$).